

PROJECT FINAL REPORT

Grant Agreement number: 222992

Project acronym: *BRAINCAV*

Project title: Non-human adenovirus vectors for gene transfer to the brain

Funding Scheme:

Period covered: 4,5 years from 01/10/2008 to 31/03/2013

Scientific representative of the project's co-ordinator¹, Eric J Kremer

Title and organisation: Director of Research Inserm, CNRS

Tel: (33) 4 3435 9672

Fax: (33) 4 3435 9634

E-mail: eric.kremer@igmm.cnrs.fr>

Project website: <http://www.braincav.eu/>

¹ Usually the contact person of the coordinator as specified in Art. 8.1. of the Grant Agreement.

4.1 Final publishable summary report

Executive summary

Prevention and treatment of diseases that affect the brain will remain formidable challenges for years. Yet, as suggested by recent clinical trials, “gene therapy” offers substantial potential and reason to believe that we can develop long-term, effective therapies for some brain diseases. Gene therapy is an approach that, instead of using classic methods (i.e. chemicals, surgery, radiation) uses DNA or RNA as drugs. Notably though, this strategy also has its own unique obstacles and risks - in particular the need to address feasibility, efficacy and safety. **BrainCAV**’s foundation is the ability of a virus called “CAV-2” to deliver DNA to neurons - the most fascinating cells in the body. To determine if CAV-2 vectors have a clinical use for therapy for brain disorders the consortium used approaches that spanned basic research through pre-clinical model feasibility, efficacy and safety. Our specific objectives included trying to understand the interaction of CAV-2 with fluid and cells of the brain. Does CAV-2 negatively affect neuron function or modify the genes that are expressed? Does CAV-2 leave the brain and go to other tissues? Does it interact with other cells besides neurons? Why do we primarily see neurons modified? How does it spread throughout the brain? We addressed these questions and have had encouraging results concerning the safety and biology of CAV-2 vectors. Convinced that CAV-2 vector deliver to the brain could be therapeutic, we treated mice and dogs that have a rare disease similar to one found in children (Sly Syndrome). Our results showed correction of many of the anomalies associated with the disease in the brain. On the other end of the scale, we also tried to better understand Parkinson’s disease, the second most common inherited brain disease in Europe. We created animals with Parkinson’s disease and we can now test therapies on these animals. Our encouraging results spurred the development CAV-2 as a bona fide drug – i.e. to make CAV-2 vector in a cost-effective, manufacturing process that satisfies the requirements needed to treat patients. Due to this EC initiative, our multidisciplinary fundamental and applied research project brought together experts from fundamental health domains such as virology, neurobiology, bioprocessing, vector production and immunology, with clinicians to identify therapies for neurodegenerative disorders. Our results should have long-term impact on the patients, families and health care system touched by some brain diseases, as well as scientist who want to better understand the biology of neurons and their functions in the brain

Project context and objectives

Our objectives were to bring a novel viral vector "from bench to bedside". **BrainCAV** tackles gene transfer to the brain by turning a virus into a vector capable of helping us understand fundamental neurobiology questions, disease progression and address therapy for global and focal brain disorders affecting children and the aging population. Our multidisciplinary fundamental and applied research project initiated a European-lead breakthrough to the domain of gene therapy for diseases affecting the brain.

Our scientific objectives are distributed into five complementary and intertwined work packages:

- To understand and define the interaction of canine adenovirus serotype 2 (CAV-2) with fluid and cells of the brain and periphery
- To use a transcriptional analysis to better understand the effects of CAV-2 vector interaction with neurons
- To test a therapy for an orphan neurodegenerative diseases commonly affecting the entire brain of children
- To develop genetic, long-lived Parkinson's disease animals and to treat its focal neurodegeneration
- To develop processes to produce and purify vectors that could bring this vector platform to the doorstep of clinical trials

Each viral vector has its specific advantages and drawbacks such as cloning capacity, memory or induced immunity, toxicity, specificity, safety, titre, or efficacy. If one wanted to genetically modify neurons the vector should preferentially transduce these highly differentiated cells, which make up ~10% of the primate brain. The advent of helper-dependent (HD) human adenovirus (HAd) vectors in the late 1990's, led to nontoxic, concentrated, homogenous preparations. HD Ad vectors also poorly integrate into the host genome, yet lead to long-term (at least 3 yrs) expression in many tissues in numerous immunologically naïve animals. The significant cloning capacity (>30 kb) also allows one to subclone an entire gene (versus a cDNA) and include numerous transcriptional regulatory elements. These advantages make HD vectors ideal for long-term gene transfer to post-mitotic cells like neurons. In 2004, we demonstrated that CAV-2 vectors have numerous advantages for clinical gene transfer, and more specifically for treatment of neurodegenerative disorders. Our proposal was designed to critically assess these advantages, the efficacy of the vector and its safety. Some of the principle characteristics and advances of the CAV-2 vector platform are:

- They preferentially transduce neurons *in vitro* and *in vivo* in numerous species
- They circumvent the ubiquitous human anti-Ad memory immune response
- They likely have a minimal effect on neurons
- They are capable of long-term expression

With these characteristics in mind, we define some of the areas in which CAV-2 vectors could be improved. We proposed a work plan to advance HD CAV-2 vectors substantially towards clinical trials.

Some of our **basic research** questions included how these virions interact with brain cells in relation to cell attachment, internalisation, and the genomic response. For example, "what cells will be transduced and why" was a simple concept for years. Now we realise that the direct interaction of vectors with cells may be a simple pathway *in vitro*, but this interaction is significantly more complex *in vivo*. WP1 was designed to address these questions. The interaction with serum and cerebral spinal fluid (CSF) will dictate and explain the ultimate location of injected particles. Then, once the vector attaches to the target cell (neurons for CAV-2 vectors), we need to better understand how the virion used axon transport to reach the neuron's nucleus.

Many viruses have been selected naturally for their ability to make progeny. Setting the cell up for replication, e.g. perturbing genes involved in cell cycle, is something even vectors initiate. The interaction between the cell and virus also leads to the induction of transcription from a subset of endogenous genes. The cell can, in turn, respond to some of these stimuli by e.g. self-destruction (apoptosis) or inducing an immune response. Who wins this tug-of-war depends on numerous factors. This critic part of gene therapy has led us to propose a global transcriptome analysis to understand the vector-cell interaction at a genetic level.

At the **applied research** level, we used the characteristics of HD vectors to demonstrate proof-of-efficacy in the healthy and diseased brain of rodents, dogs and primates. We chose two models: a rare monogenetic disorder affecting the entire brain and a relatively common brain disorder that affects a pair of nuclei. We treated the neurodegeneration caused by mucopolysaccharidosis type VII, a lysosomal storage disorder, in a 400 mg mouse brain and a ~200-fold larger dog brain. Lysosomal storage disorder are a collection of ~60 orphan diseases, primarily affecting children. Most of these disorders result from deficiencies in enzymes normally implicated in the catabolism of macromolecules inside lysosomes. No adequate option is available for the treatment of the debilitating symptoms of neurodegeneration, which is a common pathology in the majority of these

orphan diseases. Our challenge was distributing the enzyme throughout the brain. Something CAV-2 vectors were particularly efficient at doing.

We also used HD CAV-2 vectors to better understand, and possibly treat, Parkinson's disease by attempting to create genetic models (in contrast to the acute drug-induced models) that mimic disease progression. Parkinson's disease, one of the most common neurodegenerative disorders, is a chronic, progressive neurodegenerative movement disorder. It primarily affects dopaminergic neurons in substantia nigra (SN) leading to the loss of dopamine in their prime target area, the striatum. Disease modifying therapies are not available, partly, because no adequate animal model exists with chronic degeneration of dopaminergic neurons and a robust behavioural phenotype. In WP4 we will also combine the genetic- and drug-induced models to complement our understanding of Parkinson's disease and its potential therapies.

Finally, we used our bioprocessing expertise to produce and purify HD CAV-2 vectors in a streamline good laboratory practice process to make the production user-friendly and available to research laboratories. This accessibility allowed other laboratories to understand and treat other neurodegenerative disorders as well as addressing fundamental biological questions.

Results/foregrounds

BrainCAV was divided into five S&T work packages. The results are presented and discussed in the format of the respective deliverables.

WP1 - The interaction of CAV-2 with fluid and cells of the brain and periphery

WP1 was designed to further understanding CAV-2 biology in the host and assess pertinent interactions of the virus with the host, for future gene therapy at the preclinical and, ultimately, clinical levels. All deliverables were successfully submitted.

Deliverable (D)1.1: Report describing histological analysis of CAR expression in the primate brain.

We compared by immunoblotting the level of CAR expression in the adult primate versus embryonic brain. We found that in addition to a reduced level of CAR expression, CAR ran at different molecular weights suggesting a post-translational modification. We extracted protein from different regions of the primate brain and probed for CAR. Variable levels were found, which is consistent with results in the rodent brain as determined by mRNA content and immunoblotting. We used immunofluorescence (IF) to detect CAR expression in the microcebe brain. CAR was preferentially found on neurons in the soma and axons. We also looked for CAR expression at the primate neuromuscular junction. CAR was detected on the pre-synapse side and not on the muscle as previously reported.

Summary: CAR expression in neurons from the primate CNS was determined using biochemical and histological assays. Compared to data from rodents, CAR expression is similar, but not identical. CAR appears to be primarily expressed on neurons in the brain and not on glia. And while the levels decrease in older animals, CAR was still present and its expression pattern was consistent with CAV-2 tropism.

D1.2 To create a CAV-2 vector containing CAR-ablated knob and D1.3: Report comparing CAV-2 and CAV-2 CAR-ablated and in vivo

The CAV-2 fibre knob (FK) mutated in CAR binding site was tested on primary motor neurons. No specific binding could be detected compared to the native FK, suggesting the tropism of CAV-2 was CAR dependent. We therefore set out to generate a CAV-2 CAR-ablated vector to test the hypothesis that CAV-2 was CAR-dependent. We generated a CAR-binding ablated CAV-2 genome with the mutation R384E in the fibre. Homologous recombination was used to generate CAR-binding ablated CAV-2 vectors. With this aim, we generated shuttle plasmids containing the CAV-2 fibre protein. For the generation of the shuttle plasmid, we amplified a DNA fragment containing the CAV-2 fibre

protein. We introduced the modification R384E in the shuttle plasmid and finally, we generated the CAR-ablated CAV-2 virus by homologous recombination between the shuttle plasmid (including the R384E mutation) and the CAV-2 genome. Viral genomes were analysed by sequencing and restriction enzymes. While a wild type CAV-2 genome with a mutation in the CAR binding domain is interesting, it could not be used for in vitro or in vivo analysis without the inclusion of a reporter gene and/or a deletion in the E1 region. It was therefore necessary to make an E1-deleted CAV-2 vector (i.e. not virus) containing a reporter gene (e.g. GFP). Two strategies were used to create CAR-ablated CAV-2 vectors. However, the insertion of the mutated fibre sequence into CAV-2 genome was unsuccessful after numerous attempts. We then tried a second approach using bacterial artificial chromosomes (BACs) and bacterial phage recombinases. Again, after several attempts we didn't succeed.

Corrective action: We therefore created an alternative approach by addressing CAR interaction at the surface of the cell – instead of in the virus. To do this we crossed Nestin-Cre mice with mice that had the second CAR exon flanked by loxP site. This approach created mice that lack CAR in the adult mouse brain. We then generate primary culture cultures of neurons and incubated them with HAd5GFP and CAVRFP (DsRed2). We found a significantly reduced transduction efficiency of CAV-2 especially for the transduction of neurons. HAd5 transduction was modestly impaired and cells with glia morphology were transduced. These data suggested that CAR was largely responsible CAV-2 tropism in vitro. We then injected CAVGFP into the CNS of C57BL/6 and CAR CNS^{-/-} mice. We found a significantly reduced transduction at the site of injection in CAR CNS^{-/-} mice of as well as via axonal transport compared to control C57BL/6 mice, again suggesting that CAR plays a major role in the tropism of CAV-2 vectors in vivo.

Summary: Instead of addressing the role of CAR at the level of the vector, we addressed its role using a genetically induced deletion during development. We tested CAR-depleted neurons in vitro and in vivo and found that CAR plays the most significant role in CAV-2 transduction.

D1.4: Report describing axonal CAV-2 transport in neurons

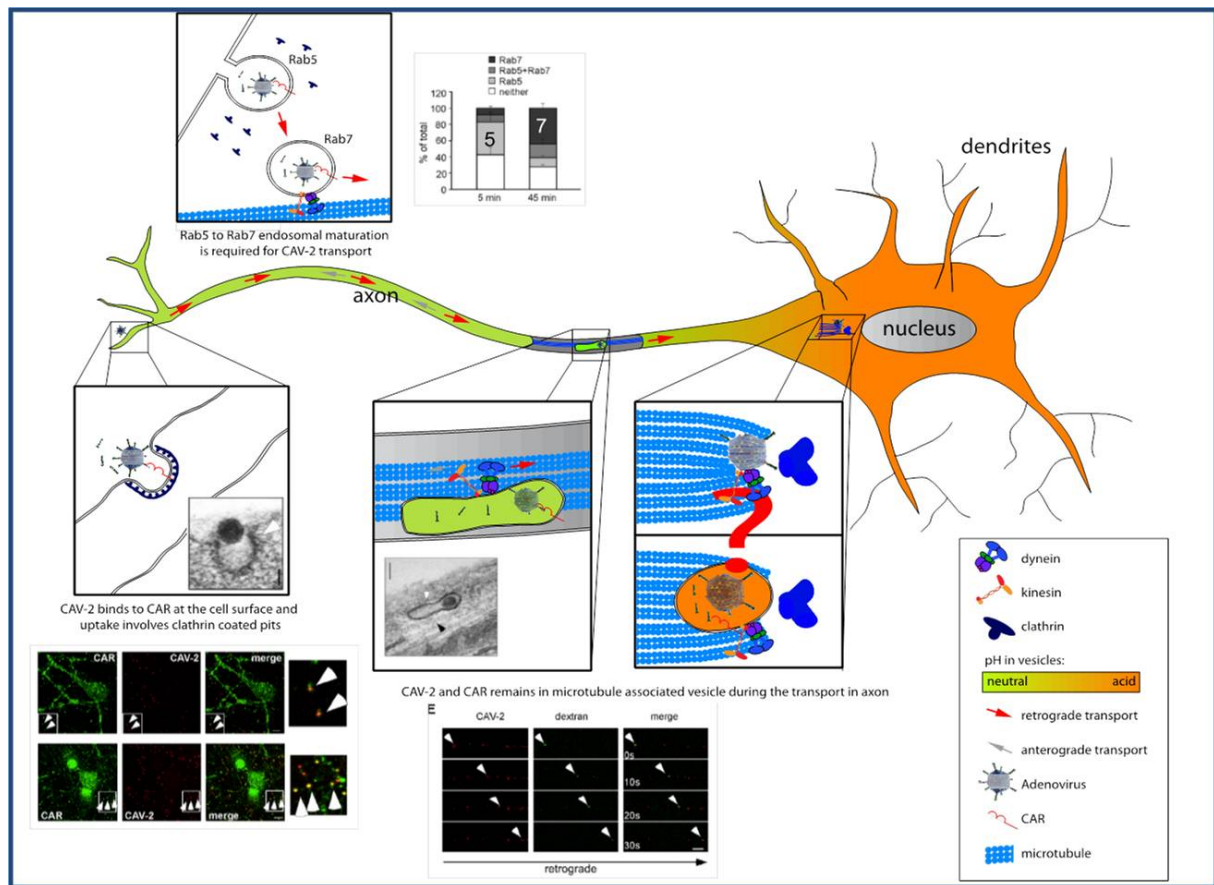


Figure 1 Schema showing the different steps of CAV-2 transport (reported in Salinas et al *PLoS Pathogens*, 2010).

First, the virus binds to CAR at the cell surface followed by internalization in clathrin-coated pits. Panel **A** upper part shows electron microscopy of CAV-2 in a coated pit; lower part shows colocalisation of CAV-2 and CAR at the surface of motor neurons. During entry, maturation of CAV-2 containing vesicles occurs, with a shift from Rab5 to Rab7 endosomes that will eventually lead to CAV-2 axonal transport. Panel **B** shows quantification of colocalisation between CAV-2, Rab5 and Rab7 during internalization. Despite Rab7 maturation, the pH of axonal endosomes stays neutral, and CAV-2 remains inside vesicles during transport. Panel **C** shows electron microscopy of CAV-2 at late stage of endocytosis, when the transport occurs, and live-cell imaging of co-transport of CAV-2 and the endocytic marker dextran. CAV-2 traffic appears to have a bias for the retrograde direction and both dynein and kinesin are involved. Unexpectedly, CAR was also found in CAV-2 positive vesicles.

Summary: The pathway that CAV-2 uses to enter and be transported in neurons was described at the molecular level.

D1.5 CAV-2 vector biodistribution in primates following stereotaxic injection

CAVGFP was injected into the striata of 7 microcebes. 4 animals were sacrificed 5 h postinjection and 3 animals were sacrificed 5 days postinjection. Brain regions and peripheral tissues were analyzed for vector genome biodistribution analysis and GFP mRNA quantification. At the 5 h very few vector genomes were detected in peripheral tissues compared to brain tissues. There was evidence of retrograde transport of CAV-2, with significant quantities of genomes in areas distant from the injection site (frontal cortex, olfactory bulb and diencephalon). Vector genome levels were highest surrounding the injection site. At the 5 days, few genomes were detected in peripheral tissues. Similar to the animals, in particular at the injection site. Vector genomes were also detected in areas distant from the injection site 5 days after administration. qRTPCR quantification of GFP mRNA expression in brain regions 5 days post-stereotaxic injection showed a broadly similar transduction profile to the vector genome distribution profile. To further assess vector genome distribution and transduction by CAV-2 after stereotaxic injection, we injected a two microcebes with CAVGFP. 3D reconstruction of GFP+ cells quantified in distinct regions of the CNS generated a global view of transduction efficacy (see Figure 2).

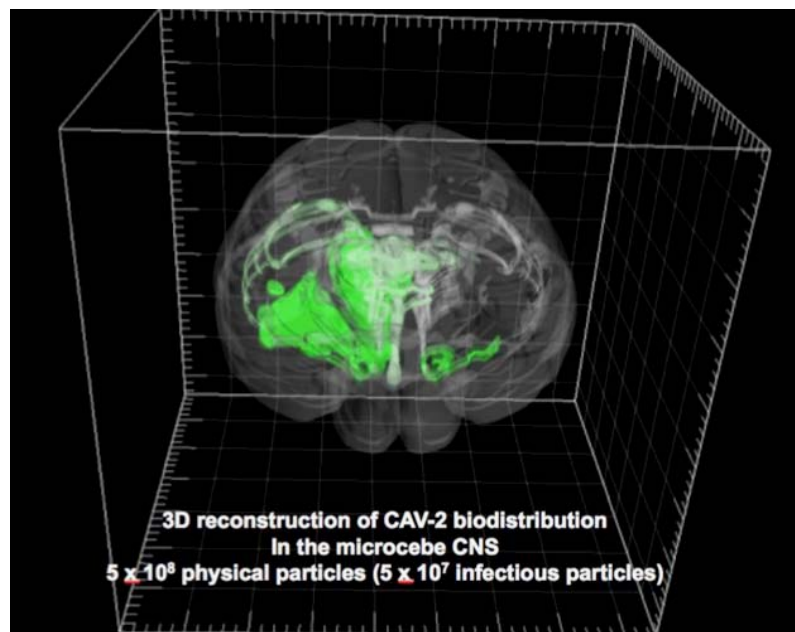


Figure 2: 3D reconstruction of CAV-2 biodistribution in the microcebe CNS

Conclusion: We assessed the genome biodistribution and transduction profiles of vectors after striatal, stereotaxic administration to microcebes. Highest levels of CAV-2 genomes, GFP mRNA and protein expression were observed in and around the injection site, although vector genomes, GFP mRNA and GFP+ cells were also detected in areas distant from the striatum.

D1.6 Proteomic and biochemical characterization of CAV-2 interactions using human blood and CSF

To complement D1.5, we assessed the interaction of CAV-2 with human serum and CSF components, using HAd5 as a control. SPR analysis of blood coagulation factor X (FX) binding to CAV-2 was carried out. HAd5, which binds FX at nanomolar affinity, was used as a positive control. SPR assays showed clear binding of HAd5 but no binding of CAV-2. *In vitro* binding experiments were then carried out in SNB19 human glioma cells and DKZeo cells to analyse the effect of blood coagulation factors X or IX or heparin on binding of CAV-2 to the cell surface. Neither FX nor FIX had an effect on binding of CAV-2 to the cell surface, although minimal binding inhibition was observed in the presence of heparin. *In vitro* cell binding experiments using an enzyme that cleaves HSPGs (Heparinase III) showed that heparin inhibition of CAV-2 binding was due to prevention of binding to HSPGs but not to CAR, which appeared unaffected by Heparinase III pretreatment by FACS analysis. Although these data suggested that there may be CAR-independent interactions of CAV-2 with the cell surface, these are likely to be of very low affinity and may be specific to the cell types that were used for the *in vitro* assays.

HAd5 interacts with several serum proteins. To identify potential CAV-2 interacting partners in pooled human serum or CSF samples, we carried out magnetocapture pull-down assays, using whole, biotinylated CAV-2 particles to co-precipitate interacting serum and CSF proteins prior to separation by 1D gel electrophoresis and identification by tandem mass spectroscopy. We found high-abundance albumin and IgG proteins. To identify potential low-abundance interacting proteins, samples were processed using an albumin and IgG-depletion kit. We analysed serum and CSF proteins magneto-captured using biotinylated virus as bait. As several putative interacting serum proteins for HAd5 have previously been characterised, HAd5 was used as a positive control for the human serum assays. Several high-abundance proteins were identified across all fractions, at satisfactory levels of confidence, including serotransferrin and α -1-antitrypsin. In addition, known interacting serum protein partners for HAd5 were identified in co-precipitates, including complement proteins (CO3, CO4A) and transthyretin. Interestingly, more proteins were identified in CAV-2 co-precipitates compared to HAd5 co-precipitates. Moreover, CO3 and CO4A also co-precipitated with CAV-2, suggesting that some adenoviral interactions with serum proteins may be conserved across species.

Summary: CAR is likely the primary functional receptor for CAV-2.

WP 2 High-throughput transcriptional analysis of HD CAV-2 effects on brain cells

Objectives: WP2 was designed to further understanding CAV-2 biology in the host and assess interplay of the virus with the host genome. All deliverables were successfully submitted.

D2.1: hNPCs transcript alterations induced by CAV-2, HAd5, AAV9 & HIV-1 vectors

Human neural precursor cells (hNPCs) were used as a *in vitro* model to test the molecular effect of HD CAV-2 on the neuron. We were interested in the absolute evaluation of gene expression following vector transduction, to identify its molecular toxicity, and in its relative quantification, to establish how CAV-2 performed compared to other viral vector candidates for neuronal therapy. hNPCs were incubated with the four vectors, i.e. 2 h at an MOI of 1000 vector genomes/cell with CAV-2, HAd5, AAV-9 and HIV-1.

Affymetrix HG U133 gene chip analysis was performed on RNAs extracted from infected and mock samples at 2 h and 5 days post infection. CAV-2, HAd5, AAV-9 and HIV-1 all modulated the 2D neuronal transcriptome, at 2 h and 5 days posttransduction. To interpret the significance of the modulation, genes that were significantly altered were analyzed with Ingenuity software. The most modulated molecular and cellular functions induced by CAV-2 were evident at 5 days postinfection and include cell cycle, cellular assembly, replication and recombination modulations. Elaboration of IPA data indicated that three major cellular pathways were variably affected: the immune response, the DNA-damage response and the pathways involved in cell trafficking. Particularly notable is the difference between CAV-2 and HIV-1 vectors for what concerns the induced modulation of the DNA damage pathway. The transcriptome variations include 182 commonly modulated genes, with 14% of the genes belonging to the DNA damage pathways modulated in opposite directions. To validate the biological information based on the extended chip analysis we performed qPCR on 24 genes and evaluated the Pearson correlation value (0.72). This indicated the reliability of chip data for the biological evaluation of neuronal response to CAV-2 and to the other viral vectors.

Summary: CAV-2, HAd5, AAV-9 and HIV-1 affect the neuron, independently from the efficiency of GFP expression. All vectors affect immune response, DNA damage and cell trafficking pathways. Particularly evident was the contrasting modulation of the DNA damage response by HIV-1 and CAV-2 vectors.

D2.2: Gene expression alterations induced by CAV-2, HAd5, AAV-9 and HIV-1 vectors in 3D cultures of hNPCs

To test the variations of the CAV-2 effects in 3D neuronal cultures, neurospheres of **hNPCs** and CAV-2 vector infection in that system were established. A full description of the methodology was published (Brito et al Methods 2012).

Differentiated neurospheres were incubated with CAV-2, HAd5, AAV-9 and HIV-1 at the fixed conditions applied to 2D cultures and described in D2.1. The relative efficiency of transduction in 3D cultures was maintained for CAV-2, while reduced for the other vectors, suggesting that CAV-2 can possibly penetrated the neurospheres more efficiently than other viral particles. RNA was extracted from neurospheres and modulation events were analyzed both by gene chip and by qPCR. After RMA normalization and T-test comparisons ($p < 0.05$), 331 and 127 genes were found significantly modulated, respectively at 2 h and 5 days postinfection. Genes were submitted to IPA and the most significantly modulated pathways reported. Compared to the 2D system, CAV-2 effect on neurospheres includes the modulation of the DNA damage response pathway, and has a milder effect on the immune system and a more significant effect on the trafficking pathways. Particularly significant of this last aspect is the modulation of CD44, which has been suggested to contribute to HAd5 entry into cells and that of caveolins.

To evaluate the relative effects of different vectors on neurospheres, specific gene modulations were quantified by qPCR. Concerning the immune system, the analysed genes were not significantly modulated, except for TLR3 and TLR4 at 2 h. Interestingly, DNA damage genes, including RAD51 and BIRC5 have opposite modulation profiles in CAV-2 and HIV-1 transduced neurospheres. This is consistent with the different genome structure, and genome related DNA damage response of the two viruses and with the data obtained in 2D neuronal cultures.

Summary: The 3D system was a valuable tool for the analysis of neuronal function. The analysis of infected neurospheres confirmed specific modulation events observed in the 2D system, including DNA damage response activation. The efficiency of CAV-2 transduction in 3D neurons and the complementary modulation of genes involved in cell trafficking, suggest that this culture method should be exploited for further studying the neuronal trafficking processes following pathogen infections.

D2.3: Report of gene expression alterations induced by CAV-2, HAd5, AAV-5 and HIV-1 vectors in human glia and neurons

A notable effect of CAV-2 on neuronal cultures is the modulation of the DNA damage pathway. We analysed the genes modulated by CAV-2: BIRC5, BRCA2, FANCD2, MRE11, CHEK1, FAS, p53 and RAD51. The induction of RAD51, MAD2L1, BIRC5 and of FANCD2 was highlighted also by qPCR. Together, these data reinforce the principle of the significance of this pathway in the response to Ads, and suggest that, in a clinical perspective, it will have to be evaluated whether and to what extent viral vectors induce, through the activation of the DNA damage response, irreversible cellular toxicity. An aspect that was relevant in the analysis of vector toxicity in a clinical perspective is the evaluation of the immune response. This analysis is also expected to contribute to studies concerning the biology of neurons whose immune function is currently being determined. We thus evaluated the genes modulated by the four vectors in 2D neuronal cultures and identified commonly modulated probes like TLR3 and TLR4, CD44, CASP1 and HAS3. To support the reliability of the results obtained through chip analysis TLR3, TLR4, HAS3, IRF3 and CD44 modulation was quantified by qPCR. These genes were induced by CAV-2 infection suggesting that neurons can activate a response to pathogens, and this appears to occur even when the pathogen, as CAV-2, was attenuated. To evaluate the response of the second component of neurological tissue to viral vectors, we set up differentiation and infection conditions of glial cells. Consistent with poor CAV-2 transduction of the glia, qPCR analysis of single gene modulation showed that this cell type is not significantly affected by CAV-2 vectors under these conditions.

Summary: A detailed analysis of the transcripts modulated by CAV-2 in neurons showed, in the cluster of immune response, the upregulation of TLR 3 and TLR4 at the late time point, along with HAS3 (the enzyme involved in the synthesis of hyaluronan (HA)), CD44, (the HA receptor) and of IRF3. Taken together, these data suggest that CAV-2 induces the activation of gene program of antiviral innate immune response. CAV-2 induces as well a DNA damage pathway with the specific modulation of genes involved in ATM signalling (p21, BIRC5, MAD2L1) and in homologous recombination (FANCD2, RAD51). Glial cells are poorly transduced by CAV-2; consistently, the level of transcript modulation induced by CAV-2 was modest in these cells.

D2.4 Gene expression alterations induced in the primate brain

CAV-2 reaches the cell nucleus via retrograde axonal transport. To better understand the effects induced by the presence of HD-GFP *in vivo*, a transcriptomic study was performed in the brain of *Microcebus murinus*.

CAV-2 was introduced in the right caudate nucleus of 8 females *Microcebus murinus*. 2 periods were investigated for the transcriptome analyse: an acute (24 h) (4 animals) and a delayed time (28 days) postinjection (4 animals). The left caudate nucleus received the PBS vehicle. For controls, 4 animals were naïve for the virus. As the striatum receives synaptic terminals from different brain structures (cortex, SN, thalamus, contro-lateral side), we assayed changes in gene expression induced by HD-GFP in the striatum and in the frontal cortex. We compared the gene expression in the ipsilateral side with the controlateral side, and with non-injected brain samples using transcriptomic approach. Total RNA of each sample, extracted from the striatum and from the frontal cortex samples was prepared for hybridization with Affymetrix HG-133 Plus2 GeneChip. The data were normalized, converted digital intensity values were converted into cell intensity files using the Microarray Affymetrix Software 5.0 (MAS 5). MAS5 labels each transcript as “present” (P) or “absent” (A) by taking into account the average difference value calculated between the perfect match (PM) and the mismatch (MM) as detailed in the Affymetrix Genechip procedure ([www;Affymetrix.com](http://www.Affymetrix.com)). A p-value was associated with the signal intensity. For each gene, the mean signal was calculated for each group. The overall rate of genes with the “present” detection call was about 18%. Moreover, we noticed a lowest SD (6%) in all the samples studied suggesting a homogeneity of the gene expression. The procedure is described below. We detected 14,400 transcripts to analyze.

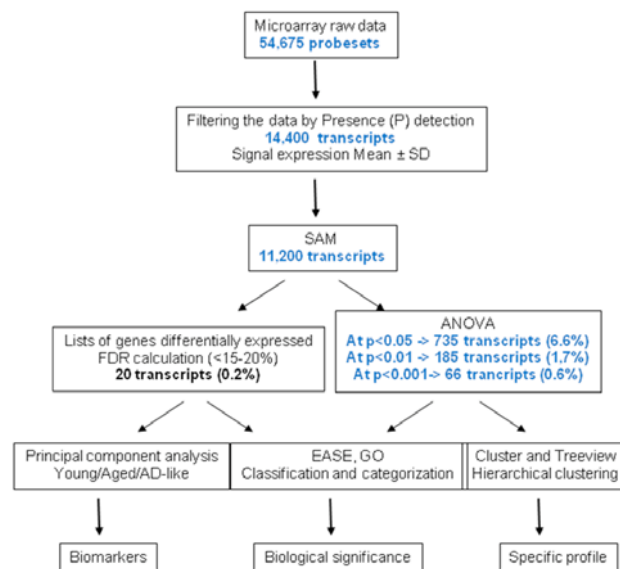


Figure 3. Schematic representation of the different analyses: Microarray data were filtered to detect the present transcripts (P). Then, the filtered data were processed by SAM. An ANOVA was preformed with the “P” data and with the data sorted by SAM. Then, the selected genes were analysed by PCA. Finally, they were investigated by clustering and were classified by functional categories.

We used the significance analysis of microarray (SAM) to identify genes that were differentially expressed when comparing for a brain structure, the three groups together, right side *versus* left side *versus* control or when comparing the time after virus infection. Among the genes that presented changes in their expression, the most notable belonged to transcriptional regulation function, the cytoskeleton and synaptic transmission. In the striatum, these genes involved in immune response were detected (e.g. an overexpression for TNFRSF18 at 24 h and for HLAG, IGHM, IGLC2 at 28 days).

Summary: Our results showed that the injection of CAV-2 induced changes in gene expression and that the expression differed. In the acute phase, HD-GFP altered the expression of protein regulating the transcription but also protein involved in the release of neurotransmitter at the presynapse. These gene expression changes could transiently modify the synaptic activity of the neurons. In the chronic phase, CAV-2 induced modifications in some transcripts implicated in the cytoskeleton suggesting a minor modification in cell trafficking. The presence of the HD-GFP-induced an increase of immunoglobulin transcripts suggesting a mild adaptive immune response in the brain.

D2.5: HD CAV-2 vector alterations of gene expression in vitro and in vivo

Neuronal 2D and 3D cell cultures were analysed for the common genes and pathways influenced by HD-GFP transduction. As anticipated in the previous WP2 deliverables, the cell damage/cell cycle and immune response pathways were modulated in both systems. The cell trafficking functions, conversely, were mainly modulated by HD-GFP infection in the 3D neurospheres. When considering the significantly regulated genes together (2D and 3D neuronal results at 5 days post-transduction), 54 probes were commonly modulated in the two systems, corresponding, respectively, to 7.7% of the genes modulated in the 2D system and to 42.5% of the 3D system. The commonly modulated genes analysed and showed that the cell cycle/ DNA damage and cell morphology functional categories were modulated in the 2D and 3D neuronal systems in the same direction (mostly, probe upregulation).

We also studied HD-GFP effect on the neuron by comparing the in vitro (2D and 3D neuronal cultures) and in vivo (*Microcebus murinus* brain) data. An *independent* statistical conditions applied for the analyses (detailed in the corresponding WP2 deliverable sections), we found no common genes. Given this result, to further develop the comparative study between the in vitro and in vivo systems, we designed a meta-analysis plan. This workflow was applied to the 2D, 3D data and to the *Microcebus murinus* brain derived chip results and contributed to further define the HD CAV-2 induced signature in primate neurons.

Summary: Taking into account the 2D, 3D and primate brain, we concluded that, at the functional level, HD CAV-2 affected the immune system, the cell cycle/DNA damage response (in 2D and 3D neurospheres), and intracellular trafficking (3D neurospheres). At the single gene level, 54 probes were commonly modulated by HD-GFP between the 2D, 3D, and none among 2D, 3D and primate brain. A meta-analysis based on a common statistical approach for 2D, 3D neurospheres and primate brain was developed.

WP 3 Treating neurodegeneration caused by MPS VII in mice and dogs

Objectives: Assessment of HD-RIGIE efficacy, toxicity and biodistribution in the β -glucuronidase (GUSB)-deficient mouse and dog models.

D3.1: Optimized HD-GUSB dose in the MPS VII mouse brain

The CNS and the skull of MPSVII mice are morphologically different from wild type littermates. We adjusted the injection point to obtain the maximum global transduction. For that reason, CAVGFP was injected into the striatum of 8-weeks old MPS VII mice at the following coordinates: 0,2 mm from bregma; 2 mm lateral; 3.5 mm deep (Fig. 4A). Results show GFP expression in many cells in the striatum and also in the dopaminergic neurons in the SN. No significant transduction was seen in other areas of the brain. A different cohort of animals was injected more rostrally, at +1,0 mm from bregma, 1,8 mm lateral and 3,5 mm

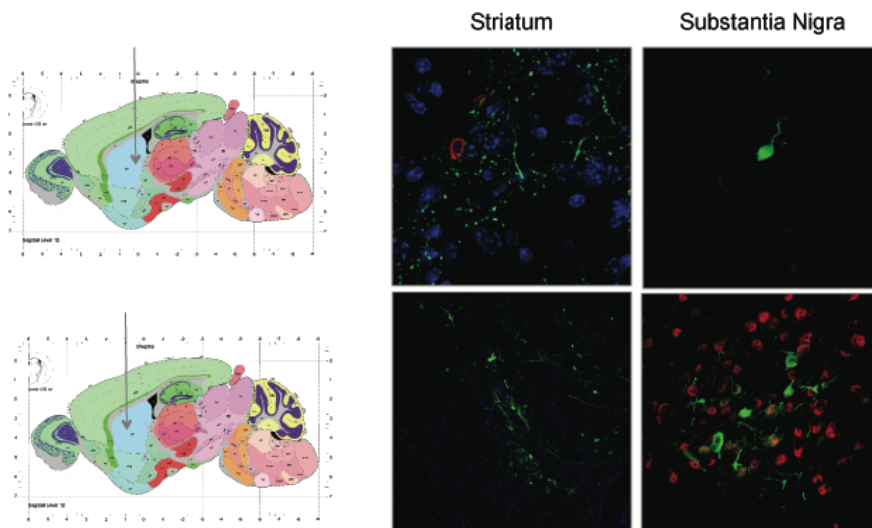


Figure 4: CAVGFP injections in MPS VII mice striatum

deep (Fig. 4B). With these coordinates, we detected GFP expression in the striatum, where the virus were injected, and in the SN, corpus callosum and cortex, where we were able to detect transduction in neurons and endothelial cells. Endothelial cells, which overexpress CAR, could have been reached

through circulation from the CSF or through microvessels present at the injection point.

Summary: We defined the following coordinates +1.0 mm from bregma, 1.5 mm lateral and 3.0 mm in depth as those that allow for more global transduction of MPSVII mouse brain.

D3.2: Optimized HD-GUSB injection site in the MPS VII mouse brain and D3.3: HD-GUSB effect based on histological analysis of the murine MPS VII brain

A group of 8 transiently immunosuppressed animals were injected bilaterally at ~9 weeks of age with 2×10^9 pp of HD-RIGIE/striatum. Control littermates (heterozygous and mutant mice) were injected with the same volume (2 μ l per hemisphere) of PBS. Mice were sacrificed at 6 weeks and GUSB activity was assayed every 100 nm. No GUSB activity was detected in PBS-treated mutant or even heterozygous mice, showing the low sensitivity of the assay. We detected transgene expression in striatum, several areas of the cortex, corpus callosum, SN and around ventricles. Overall, based on this assay, we estimated a volume transduction about 4 mm around the injection point.

Brains were sliced in 2 mm pieces and protein extracts were prepared. We performed a total of 6 slices/brain, named S1 from the olfactory bulb to S6 containing the cerebellum and brainstem. For each slice, we measured GUSB activity using a fluorometric assay, as well as β -hexosaminidase (β -hex) activity, another lysosomal enzyme that is secondary elevated when GUSB is missing. Data was plotted as the % of activity of each enzyme compared to heterozygous mouse levels, which have a completely normal quality of life. GUSB activity in heterozygous mice is 80% of the wild type animals (wt), although only 50% activity was expected. GUSB activity was not detected in mutant mice. On the other hand, HD-RIGIE-treated mice showed up to 60% of the heterozygous levels at the injection point and statistically significant activity in slides S1-S4, compared to non-treated mutant mice ($p < 0.001$). More importantly, we show an important decrease in the secondary elevation of β -hex in all brain areas, providing evidence of biochemical correction. Exact correlation between GUSB levels and β -hex activity is shown in all sections. Remarkably, no statistically significant differences were detected among treated and heterozygous mice for slides S1- S4.

MPS VII is characterized by the inability to degrade glucuronic acid-containing glycosaminoglycans (GAG). We analysed the content in GAG in the three groups of animals. We achieve reduction of GAGs in all sections of the brain, consistent with the GUSB activity and reduction of β -hex. Again, as for β -hex, no statistically significant differences were detected in GAG contents among treated and heterozygous mice for slides S1-S4, while statistically significant differences were demonstrated for all sections ($p < 0.001$). Finally, we analysed the histopathology of these mice in cortex, striatum, meninges and hippocampus at the injection point and also at more distal areas. We found significant

correction of neurons but also glial cells, more dramatically affected by distended lysosomal storage, in all areas analysed.

HD-RIGIE 6 weeks earlier. Semi-thin sections of different brain areas surrounding the injection point were stained with toluidine blue to highlight the enlargement of vacuoles containing lysosomal storage material as seen in PBS-treated GUSB mice. Representative images from (a) cortex, striatum and meninges in MPSVII PBS (left), MPSVII HD-RIGIE (middle) and WT mice (right) at injection point, and at more distal areas (b), slides S3 (left panel) and S4 (right panel) and (c) hippocampus. HD-RIGIE-treated mice show a pattern similar to wt animals in all tissues analyzed. Additional groups of 7 animals, at 8-10 weeks of age, were injected with the same experimental design and mice were analyzed 16 weeks after transduction. Similarly as it has been shown at 6 weeks, we detected β -glu staining in brain slices, extending about 12 mm around the injection (Fig. 5a).

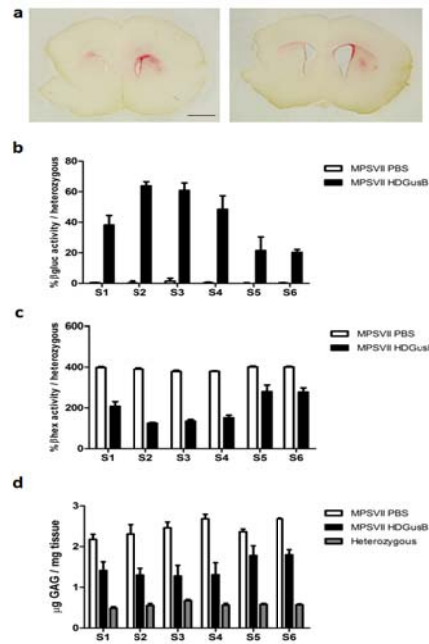


Figure 4. Enzyme activity and GAG accumulation analysis 16-weeks after the treatment. β -gluc activity in (a) 100 μ m-slides, in red (bar scale 1mm), (b) 2mm-slide homogenates and (c) β -hexosaminidase activity and, (d) GAG accumulation in 2mm-slide homogenates slides in in MPSVII mice injected with PBS or HD-RIGIE compared to heterozygous mice (n=2 for MPSVII PBS, n=2 for MPSVII HD2GusB and n=4 for heterozygous mice).

GUSB and β -hex activity and GAG accumulation on protein extracts are shown in Fig. 4b-d. Similarly as for animals euthanized at 6 weeks, we achieve significant overexpression of GUSB, particularly in slides S1-S4, correlating with a decrease in β -hex and GAG accumulation in the whole brain, showing no statistically significant differences between GUSB-treated and wt animals in S2 and S3 slices. This is especially important at 16 weeks of age, when the pathology of the disease is much more severe

and these animals are at the end of their life expectancy. Correlating with the functional correction of brain sections, histopathology of proximal and distal areas to the injection point show significant reduction of lysosomal storage in neurons and glial cells (Fig. 6). NB the dramatic enlargement of lysosomes in these animals at the end of their life.

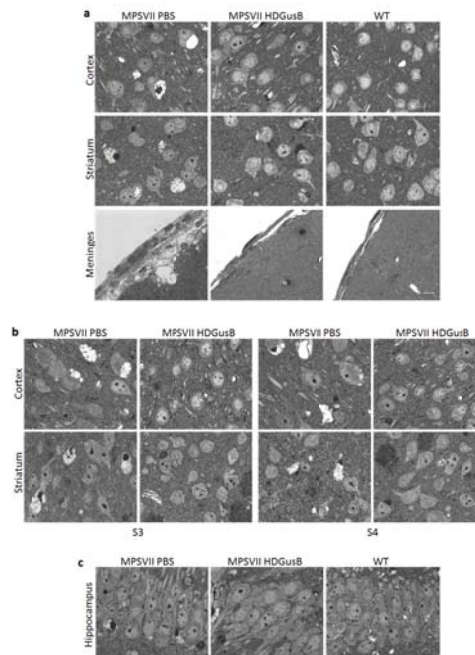


Figure 6. Histopathology showing correction of cortex, striatum and meninges of GUSB mice treated with HD-RIGIE 16 weeks earlier. Semi-thin sections of different brain areas surrounding the injection point were stained with toluidine blue to highlight the enlargement of vacuoles containing lysosomal storage material as seen in PBS-treated GUSB mice. Representative images from (a) cortex, striatum and meninges in MPSVII PBS (left), MPSVII HD-RIGIE (middle) and WT mice (right) at injection point, and at more distal areas (b), slides S3 (left panel) and S4 (right panel) and (c) hippocampus. HDCAV2-treated mice show a pattern similar to wt animals in all tissues analyzed. Scale bar, 20 μ m.

Conclusions:

1. Brain transduction using HD-RIGIE vector is able to drive transgene expression to the whole brain of GUSB mice, 6 and 16 weeks after one single injection of the vector per hemisphere.
2. One injection of HD-RIGIE allowed for short and long-term β -glu expression up to 60% of heterozygous mice and, more importantly, to complete biochemical recovery of secondary elevation of β -hex and correction of GAGs in 4 out of the 6 slides of the brain, covering the whole cerebrum with the exception of the cerebellum and the brainstem.

3. Correlating with correction of biochemical parameters, β -glu expression driven by HD-RIGIE lead to short and long-term clearance of lysosomal storage accumulation at the injection point but also in many distal areas.

D3.4: Behavior modifications following HD-GUSB injection in the murine MPS VII brain

Animals were behaviorally evaluated 6 weeks after treatment in a series of tests used as a screening for behavioral abnormalities and physical condition in mutant mice (Giménez-Llort et al., *Eur. J. Neurosci.* **16**: 547–550, 2002). The behavioral domains analyzed included physical condition, sensorimotor functions, behavioral and psychological symptoms (anxious-like behavior, exploratory activity, daily life activities) and cognitive function. Experiments were conducted between 10:00 and 17:00 h. In all experiments animals were counterbalanced per genotype and gender. The research was performed in accordance with 86/609/EEC regarding the care and use of animals for experimental procedures. Animals were weighed before each test.

MPSVII mice show poorest physical condition as compared to wt animals, which was improved by HDCAV2GUSB-treatment. Poorest daily life activities were shown in the *nesting behavior* and seemed to be also improved in HDCAV2GUSB-treated animals. The assessment of animals in an abbreviated version of *SHIRPA*, *wood* and *wire rod tests* and *hanger tests* evidenced impairment of sensorimotor functions. MPSVII animals showed lower reactivity to handling as well as poorest prehensility in the use of elements of support and strength. Visual and forelimb reflexes, motor coordination and equilibrium were normal.

The assessment of animals in a short battery of classical tests used for behavioral and psychological symptoms of dementia-like behaviors (*corner test*, *open-field test* and *T-maze*) indicated presence of neophobia and other anxiety-like behaviors and severe problems of interaction with the environment as shown by the strong reduction of exploratory activity in all these tests (Fig. 7). These behavioral symptoms were reversed by HDCAV2GUSB-treatment.

With regards to the assessment for spatial learning and memory, studies in the Morris water maze indicated that MPSVII mice have deficits in the learning acquisition process and in the total learning capacity (Fig. 8). The results in the cue learning indicate that non-treated animals can succeed in the acquisition of an easy-cued task but their total capacity is impaired. Twenty-four hours later, when the animals were assessed again in a more difficult task (place task acquisition) their cognitive abilities did not show any benefit of previous experience, as their behavior was equal as that shown in the first day of experience in the maze. In contrast, wt animals did remember the prior location of the platform and insisted to search for it. The following trials of the place task learning also indicate impairment in the short-term memory and deficits in the total learning capacity of MPSVII as compared to wt mice (Fig. 8). Treatment with HDCAV2GUSB rescued the cognitive deficits and most importantly the total learning and memory capacities.

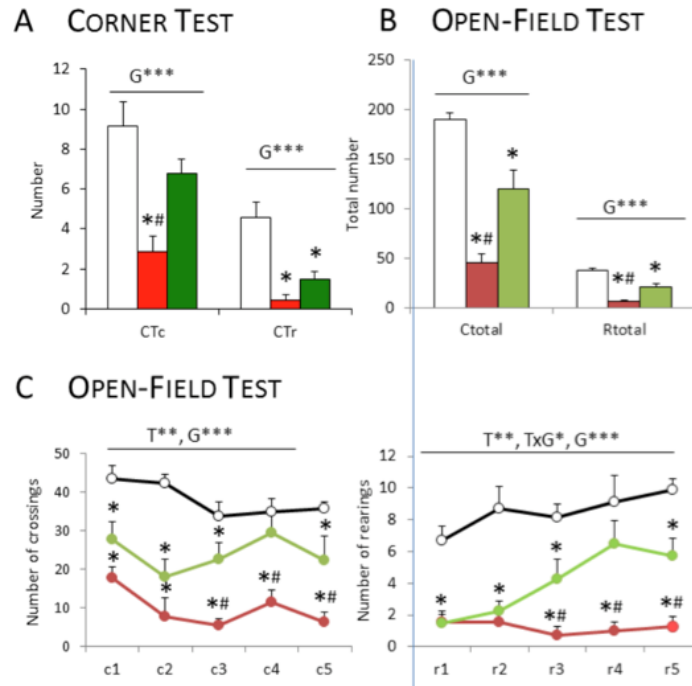


Figure 7. MPSVII mice treated with HDCAV2GUSB show reversal of anxiety-like behaviours and improved exploratory behaviour. Behavioral and psychological symptoms of dementia-like behaviors were detected in MPSVII mice using the corner test and the open field test. MPSVII mice showed reduction of total crossings and total rearing. Levels of horizontal and vertical activities are significantly improved (2-fold) by 6 weeks of HDCAV2GUSB treatment [T= time; G= group; TxG= time x group; * $p<0.05$; ** $p<0.001$; *** $p<0.0001$. Post-hoc Duncan's test, * $p<0.05$ vs. WT, # $p<0.05$ vs. HDCAV2GUSB treatment].

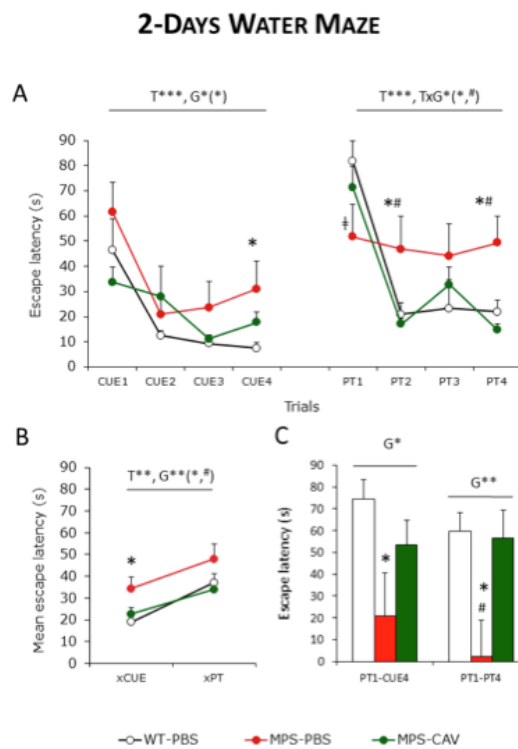


Figure 8. Effects of HDCAV2 treatment on spatial learning and memory in MPSVII mice. (A) Acquisition curves showing

latency to find the visible (CUE1-CUE4) and hidden (PT1-PT4) platform in a 2-day mouse water maze. Escape latencies through the cue-learning task was similar between groups but MPSVII showed poorest baseline performance in the last visible platform trial. In the reversal place-learning task, MPSVII mice showed significantly worse escape latencies compared to the good acquisition shown by WT and MPSVII-treated mice. **(B) Long-term memory.** Mean escape latency in the cue- and place-learning tasks. MPSVII mice showed a worse long-term performance compared to WT and treatment with HDCAV2 restored this deficit. **(C) Long term and short-term memories.** Long-term memory deficits observed in the escape latency after 24h interval (PT1-CUE4) were lacking in MPSVII-HDCAV2 animals. Short-term memory deficits observed in the place-learning task (PT1-PT4) were reversed in treated animals [T= time; G= group; TxG= time x group; * $p<0.05$; ** $p<0.001$; *** $p<0.0001$. Post-hoc Duncan's test, * $p<0.05$ vs WT, # $p<0.05$ vs HDCAV2GUSB treatment].

Summary: MPSVII animals showed impairment in all the domains studied with main affection on cognition and HDCAV2GUSB was able to successfully improve and/or reverse the major deficits including total learning and memory capacities.

D3.5: HD-GUSB effect based on histological analysis in the dog MPS VII brain

The brains of seventeen dogs were injected with HD CAV-2 vectors. The initial cohort was injected with HD-GFP to determine efficacy, level of retrograde transport, immunogenicity, neuropathology, and optimize doses and coordinates in the healthy and MPS VII dog brains. Initially, stereotactic injection in dogs, and particularly in MPS VII dogs, was challenging because of the variation in the size of pups, the lack of a detailed atlas for 2 to 3-month-old mixed breed dogs, and MPS-associated bone deformation that did not allow a trustworthy location of the bregma or brain structures. Because MRI facilities were not available to determine stereotactic coordinates, injections were targeted to large structures and, when relevant, multiple coordinates along the needle track. The above constraints certainly led to vector delivery into ventricles in some MPS VII dogs, which in this case would lead to loss of extra-chromosomal vector genomes in dividing ependymal cells. At the site of striatal injections, cells with quintessential neuron morphology were predominant. We detected GFP+ cells throughout each hemisphere in particular on the striatum; thalamus; hippocampus; frontal, temporal, occipital cortex and nuclei of Meynert. In dogs injected unilaterally, we detected GFP+ cells throughout the ipsilateral hemispheres and in the contralateral cortex, which has efferent projections to the injected striatum. To distinguish between neurons and glia we stained sections with anti-NeuN and anti-GFAP antibodies. In afferent regions all GFP+ cells were neurons, while at the site of injection the majority of GFP+ cells also expressed NeuN. Combine, these data demonstrated that CAV-2 vectors preferentially transduced neurons in the large dog brain and are capable of efficient axonal transport, which is consistent with the tropism of CAV-2 in rodent brains and in organotypic cultures of human brain biopsies.

We injected HD-RIGIE into the brain of six MPS VII dogs that were sacrificed at 1 or 4 months postinjection and sections were used to assay the biodistribution of GFP and β -glu activity. We detected β -glu activity in sections near the predicted injection sites in the hippocampus and caudate

nucleus in all brains. At 4-months postinjection, staining was notably more intense in several areas of the MPS VII brain parenchyma. We used a biochemical approach to assay to quantify β -glu activity in tissue homogenates. Consistent with the in situ β -glu assays, β -glu activity was detected in the striatum, hippocampus and thalamus. Consistent with the biodistribution of GFP expression via axonal transport, we found increased β -glu activity throughout the frontal, parietal, temporal and occipital cortexes – structures that were not targeted by vector injections. Combined, these data demonstrated the widespread distribution of β -glu activity, likely due to a combination of HD-RIGIE and β -glu transport, in a brain that was ~30% the size of a 2-yr-old child and 50-fold greater than a mouse brain. We also compared β -hexosaminidase (β -hex) enzymatic activity in healthy, HD-GFP-, and HD-RIGIE-injected dogs. β -hex activity in the striatum of most HD-RIGIE-injected dogs was significantly reduced when compared to age-match HD-GFP-injected dogs. β -hex activity in the hippocampus also returned to levels of healthy dogs in four of the six dogs injected with HD-RIGIE. More pertinent, throughout the noninjected cortex, which contains massive projections into the injected structures, β -hex activity returned to healthy levels in all MPS VII dogs injected with HD-RIGIE.

Neuropathology was then assessed by toluidine blue staining. The MPS VII dog brain injected with HD-GFP and sacrificed at 1 or 4 months had large nonstaining vacuoles. In HD-RIGIE-injected MPS VII dogs sacrificed at 1 month, we detected a reduction of nonstaining vacuoles in cells throughout the caudate nucleus, hippocampus and cortex. The majority of cells with glial or neuron-like morphology had no detectable storage vesicles and they were not different from the cells in comparable regions in healthy dogs. At 4-months postinjection of HD-RIGIE, a small minority of cells was found with nonstaining extended vacuoles in the caudate nucleus, hippocampus and cortex. Together, these results are consistent with the β -glu activity assays and correction of MPS VII neuropathology.

The intensity and distribution of neuropathology in dogs injected with HD-GFP and HD-RIGIE was then graded. In HD-GFP-injected dogs, the masked observer graded all regions as severe. In the four HD-RIGIE-injected dogs sacrificed 1 or 4-months post-injection, global neuropathology was generally mild or moderate but in some regions neuropathology remained severe. In M2599, the final dog in this study, neuropathology was globally mild with some regions still moderate. To complement the results showing reduced GAG storage in HD-RIGIE-injected dogs, we also assayed for LAMP1 expression, a marker of lysosomes. Like β -hex, LAMP1 is overexpressed in the MPS VII cells via TFEB master regulation. In addition to the increased expression, one can detect larger LAMP1+ vesicles in MPS VII cells. In healthy dog brains, LAMP1 expression was in small punctate structures. Throughout

the HD-GFP-injected MPS VII brain, LAMP1 expression was notably more intense and associated with larger structures. In HD-RIGIE-injected brains, LAMP1 staining resembled the strength and pattern present in healthy brains. As above, this improvement was also found throughout the cortex, a regions that did not receive direct HD-RIGIE injections. Combined, these data further supported our conclusion that HD-RIGIE improved the neuropathological hallmarks of MPS VII in dog brains.

Conclusion: we assayed the efficacy of a HD CAV-2 vector containing a human GUSB expression cassette in the canine young MPS VII brain. As little as $\sim 2 \times 10^8$ infectious particles of HD-RIGIE led to histological improvement throughout the MPS VII dog brain. A striking result was the comparable efficacy of HD-RIGIE: the dose injected into the MPS VII dogs was 50 to 200-fold lower than that used for AAV vectors in the brains of Sanfilippo and Hurler syndrome dogs. To put this dose into a more global gene transfer perspective, it would not be surprising to see 8×10^9 physical particles of a HD vector used in the rodent brain. Equally clinically relevant, and in contrast to studies using AAV vectors for MPS therapy, only transient immunosuppression appeared necessary and we found no obvious reduction in efficacy in the MPS VII dogs that were sacrificed 4 versus 1 month postinjection.

D3.6: Behavior modifications following HD-GUSB injection in the dog MPS VII brain

Due to the severity of the joint and cardiac problem associated with MPS VII in these dogs we were unable to assay behaviour modifications associated with brain gene transfer. Eventually this could have been overcome with β -glu enzyme replacement therapy, but the costs, limited supply of enzyme and minimum time postinjection did not allow this.

WP4: Developing novel genetic Parkinson's disease models & treating neuron death

Objectives: i) characterize the biological functions of LRRK2; ii) establish a high-content cell-based array for drug development; iii) develop models for Parkinson's disease using ectopic expression of wild type and mutant LRRK2; and iv) test the efficacy of HD CAV-2-mediated delivery of GDNF for neuronal protection against acute and genetically-induced parkinsonism.

D4.1 Report describing HD-LRRK2 vector efficacy in hmNSCs

In the CNS of rodents, dogs and primates, CAV-2 vectors preferentially transduce neurons when injected into the parenchyma. Whether CAV-2 vectors also transduce precursors of human brain cells that maintain the potential to differentiate into neurons or glia was unknown. To address this, we assayed human neural stem cells (hNSCs), which can be derived from specific brain regions and give

rise to specific neurons such as dopaminergic neurons, when tissue is derived from fetal midbrain (hmNSCs).

We initially determine the efficacy of transduction in hmNSCs using CAVGFP, an E1-deleted vector, during proliferation and differentiation as well as establishing a dose response (physical particle/cell, pp/c). Transduction efficacy was quantified via flow cytometry. At 1000 pp/c during proliferation resulted in optimal transduction of hmNSCs without affecting viability. At 2000 pp/c more cells were transduced, but associated with toxicity. Almost all cells expressing GFP differentiated into neurons. Because HD CAV-2 vectors have a lower infectious to physical particle ratio, we tried to optimize the transduction efficacy and reduce toxicity at higher doses. As a control, we compared MDCK cells to hNPCs. These data indicate that the efficacy of HD-LRRK2 in hNPC is lower compared to that of MDCK cells. Immunocytochemistry of MDCK cells suggested that some GFP+ cells incubated with HD-LRRK2(G2019S)-GFP expressed detectable levels of LRRK2(G2019S).

Summary: While HD-LRRK2 transduced MDCK cells efficiently, hmNSCs were transduced with lower efficacy.

D4.2 Report describing the effect of HD-LRRK2 on proliferation and differentiation in hmNSCs

Vector dose of HD-CAV-2 expressing the mutated LRRK2 G2019S gene (HD-CAV-LRRK2*) was studied in undifferentiated and differentiated hmNSCs cultures, in comparison to the mock vector HD-GFP. For initial screen of transduction parameters, HD-GFP was used. Different transduction settings were assessed in undifferentiated and differentiated cultures, by combining MOIs and transduction time.

Analysis of fluorescent GFP-positive cells indicated lower percentage of transduced cells when lower MOI and short transduction time (300 pp/cell, corresponding to 100 vg/cell, 2h) were combined; the highest percentages were observed when high MOI and long transduction time (3000 pp/cell, corresponding to 1000 vg/cell, 24h) were used. Flow cytometry analysis revealed no significant differences in percentage of GFP-positive cells between proliferative and differentiated cultures (around 50% of GFP-positive cells for 3000 pp/cell, 24h); nevertheless, gene expression (quantitative qRT-PCR) and protein analysis (fluorescence microscopy and western blot), showed higher levels of GFP in differentiated cultures than in proliferative (~ 25-fold increase in gene expression). Despite the high transduction efficiency obtained using high MOI and transduction time, this was associated with higher toxicity, revealed by an increase up to 60% in PI-positive dead cells, 5 days post-transduction. Gene expression and protein analysis of tyrosine hydroxylase (TH), a specific dopaminergic neuronal marker, showed that higher MOIs impacted the expression of this marker, particularly when combined with longer transduction times (Figure below), for which a 7-fold reduction in TH expression was observed. Based on these results, HD-LRRK2* transduction was tested on undifferentiated and differentiated hmNSCs cultures, combining short transduction times with low and high MOIs and long transduction times with low MOIs.

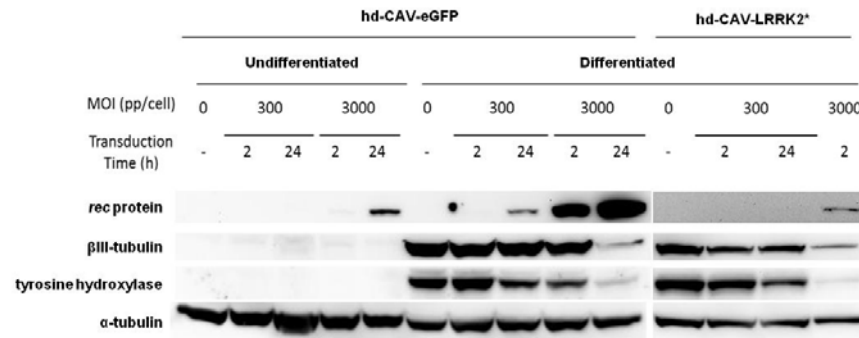


Figure 9: Characterization of transduction with hd-CAV-eGFP and hd-CAV-LRRK2*, in undifferentiated and differentiated hmNPC cultures 5 days post-transduction: (A) Western Blot analysis of recombinant protein (eGFP and LRRK2), neuronal (beta-III-tubulin), dopaminergic (tyrosine hydroxylase) markers and the loading control alpha-tubulin.

Transgenic LRRK2* mRNA and protein were detected for transduction at MOI 3000 pp/cell, 2 hours. For these transduction conditions, EdU incorporation and cell cycle analysis showed that the fraction of proliferating cells was not significantly affected by transduction with hd-CAV-LRRK2*. In accordance, expression of proliferating cell nuclear antigen (PCNA), analyzed by qRT-PCR, was not significantly affected by transduction.

Similarly to undifferentiated cells, transgenic LRRK2* mRNA and protein were detected only for transduction at MOI 3000 pp/cell, 2 h. For this condition, impact of transduction on cell viability was similar to HD-GFP, with approximately 35% of PI-positive cells detected 5 days posttransduction, as well as the impact on expression TH.

Immunofluorescence analysis of the neuronal marker beta-III-tubulin suggested that hd-CAV-LRRK2* transduction at MOI 3000 pp/cell was associated with a decrease in number of neurons and neurite length/branching (Figure below).

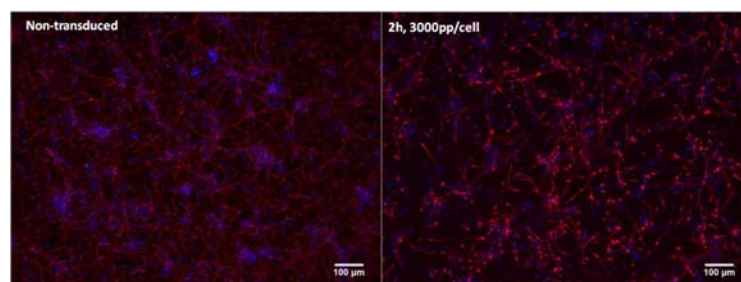


Figure 10: Immunofluorescence microscopy of differentiated hmNSCs non-transduced and transduced with hd-CAV-LRRK2* (beta-III-tubulin, red; DAPI, blue).

The transduction conditions of MOI 3000 pp/cell, 2 h, using the initial HD-LRRK2* batch, were used for 2D cultures of proliferative and differentiated hmNPC were transduced with HD-LRRK2* and HD-GFP. Cells were collected 5 days post-transduction for transcriptional analysis.

To assess the possible toxicity associated to the presence of the mutated LRRK2 protein (LRRK2 G2019S) in neuronal progenitor cells, we evaluated the expression of proliferative, apoptotic, midbrain and dopaminergic markers before and after DA differentiation.

Progenitor cells were transduced with HD-CAV-2 expressing LRRK2G2019S at an MOI of 1000 pp/cell, and compared to HD-GFP. Cells were collected 5 days posttransduction for RNA extraction and qPCR assays.

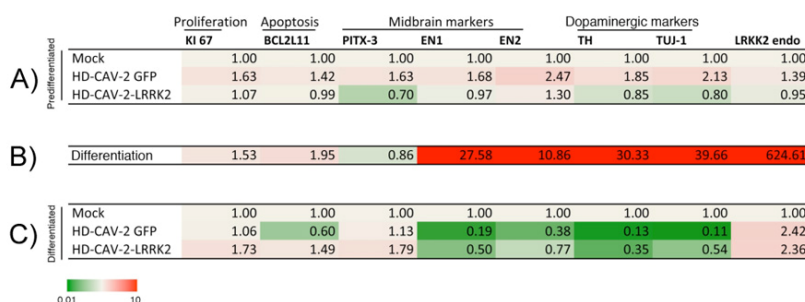


Figure 11. The fold changes values of each marker are displayed. Color gradient shows the levels of modulation, ranging from green, which represents down regulation to red, which corresponds to the upregulation, with respect to mock, indicated in grey. The values represent the mean estimate from four independent qPCR experiments.

Of note, in pre-differentiation conditions (**A**) we observed a slight downregulation of PITX-3, TH and TUJ-1 in cells transduced with HD-LRRK2 as compared to mock- and HD-GFP cells. As expected, the differentiation process induces the strong upregulation of Engrailed 1 (EN1), Engrailed 2 (EN2), TH and TUJ-1 markers, in addition it caused the increase of the endogenous LRRK2 mRNA levels (**B**). In differentiated cells, upon exposure to viral vectors, (**C**), we observed the downregulation of EN1, EN2, TH and TUJ-1. The effect was observed both in cells exposed to HD-CAV-2-LRRK2 and in HD-CAV-2-GFP treated cells, indicating an effect related to the vector treatment rather than to a specific LRRK2 G2019S toxicity.

Summary: Overall LRRK2G2019S did not induce significant specific alterations in proliferation apoptotic and neuronal markers in our cellular model.

D4.3: Report describing the cell based HCS system using LRRK2 expression in hmNSCs

Partner 8 did not perform these assays.

D4.4 Report describing HD-LRRK2* efficacy in the rat brain

The striatum of 16 rats were injected unilaterally at 2 coordinates with HD-LRRK2 and HD-LRRK2 G2019S. The controls were sham and HD-GFP injected (n = 8).

After the baseline of each individual animal was measured 3 days pre-injection by the amphetamine-induced rotation test, the rats were retested 1-month post-injection vector. We found no significant difference in the rotational behavior depending on the injected virus. At similar times, motor learning was tested using the cylinder test. Again there was no significant difference between groups. Rats were sacrificed 1-month postinjection for histological analyses. Tyrosine hydroxylase (TH)-immunoreactivity in the striatum as a measurement of dopaminergic terminal integrity was not reduced in virus injected animals. The number of TH-positive cells in the SN was also not affected. In addition, there was little GFP fluorescence in injected striata and none in the SN. Thus, we concluded that the amount of injected particles was not sufficient to efficiently transduce dopaminergic neurons in the SN and also that there was no behavioral or histological effect of such injections.

Summary: 16 rats were injected with LRRK2 containing vectors plus controls. We found no changes in the brain. Proposed corrective actions (intranigral injections, inject more particles and/or transiently immunosuppress) were not performed by partner 8.

D4.5: Report describing HD-LRRK2* vector efficacy in microcebes

The task was separate into different experiments (figure 12)

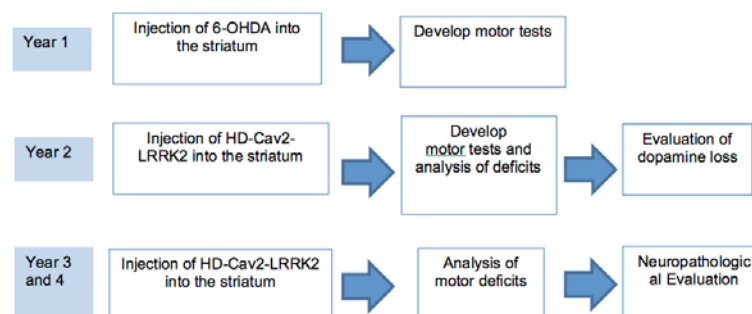


Figure 12 Experimental design to test vector efficacy in microcebes

1st year: we developed behavioural tests after the injection of 6-OHDA:

- 1) hourglass: The animal is placed in a cylinder that is turned upside down. We measure the time taken by the microcebe to return to the upright position. Usually, unimpaired animals do it in less than 3 seconds;
- 2) tower with 7 levels of rungs where the microcebes have to jump from the ground to the 7th level, and where the difficulty increases progressively
- 3) reward searching in one of 6 aligned tubes; it consisted in reward searching in one of 6 aligned tubes. The animals have to jump on a small platform to reach the reward. We measure the time to catch the reward during 30 trials and the hand used.
- 4) hill and valley staircase task.

2nd year: we performed pilot studies with HD-LRRK2* (G2019S) vectors injected in the caudate putamen of two microcebes (4.5 x 10⁹ pp, 3µl injected, coordinates A:5 mm, L: 2mm, P: 8mm, 5 mm, 4mm). The microcebes were sacrificed 15 days after injection. We then investigated the loss of dopaminergic neurons in the SN. We observed a loss of dopaminergic neurons of 24% and 42%. The behavioural study showed that we need to train the animals before injection and follow up them during all the incubation time.

3rd – 4th year: We injected unilaterally at 2 coordinates with 2 x 10⁹ physical particles of HD-LRRK2 and HD-LRRK2* G2019S (controls: 6 lemurs HD-GFP, 4 lemurs HD-LRRK2, 8 lemurs HD-LRRK2* injected). Prior to vector application, all the animals were trained to perform motor tasks. Then the mouse lemurs were followed up with behavioural tests during 6 months post-injection. At the end of the follow up, the animals were sacrificed and the brains were processed for IHC studies.

Behavioral studies

Hourglass test:

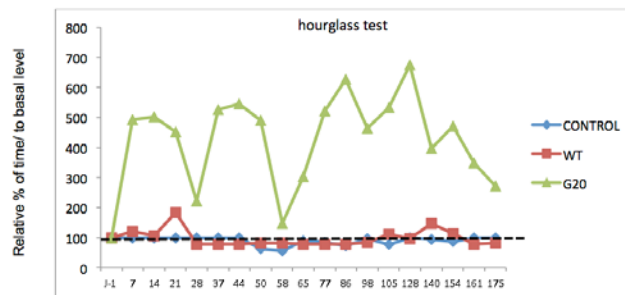


Figure 13 : performance of the mouse lemurs in the hourglass test

G2019S LRRK2 lemurs are considerably impaired from 1 week to 3 weeks after injection in the hourglass test compared to performance before injection and this deficit is observed during the 6 month follow up. The G2019 lemurs did never reach again the baseline (before injection) (Fig.13). For wild type LRRK2, the impairment occurs 3 weeks after injection, then the animals recover good performances compared to the baseline. Control animals keep baseline performance during the follow up.

Tower test

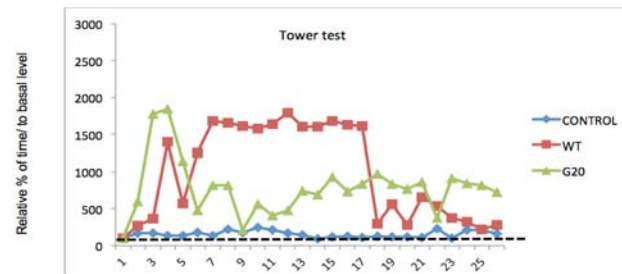


Figure 14 : performance of the mouse lemurs in the tower test

Control animals show constant performance along the follow up meaning that animals did not encounter any difficulty to jump (Fig.14). G2019S lemurs (particularly 3/8 mouse lemurs) present an important impairment 3 weeks after the injection then recover progressively during 6 weeks and

show again motor deficits along the follow up. For wild type animals, important motor deficits are observed 4 weeks after injection until 18 weeks and then the animals are less impaired but never reach again the baseline.

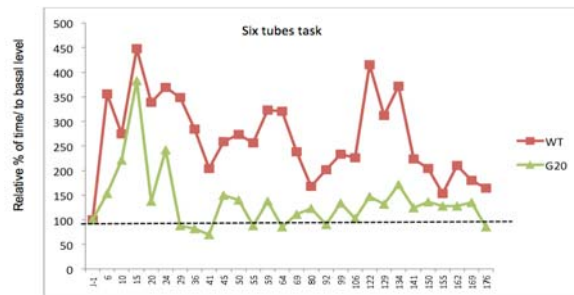


Figure 15: performance of the mouse lemurs in the 6-tube task.

The wild type lemurs were impaired all along the follow up starting 10 days post-injection (Fig. 15). The time to get the reward was 1,5 times to 4.5 times increased compared to the time at baseline before injection. The G2019S lemurs were impaired during one month with an increasing time to get the reward and then the time decreased progressively. We note that for some animals, they change the hand used to get the reward and it is the reason why they get the reward quickly again. Control animals did not want to do this test before injection.

Post-mortem studies

Histological studies were done at the end of the 6 month-follow-up. It is important to note that the behavioural impairment was not maximal at the end of protocol.

Detection of protein expression with immunohistochemistry

We have performed different labelling with various antibodies: anti-LRRK2, anti-Flag, anti-GFP to detect HD-CAV2 transduce neurones, anti-TH to detect dopaminergic neurones, anti-GFAP to detect astrocytic inflammation.

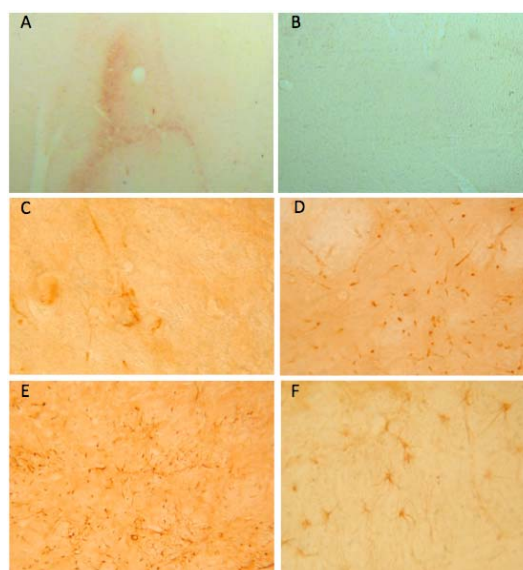


Figure 16: protein expression into the striatum and the SN

Flag, GFP and LRRK2 signals were very weak into the striatum and the SN 6 months after injection. Flag labelling was detected into the striatum 2 weeks post injection on the ipsilateral side (Fig. 16A) but not in the contralateral side (Fig. 16B) but not anymore 6 months post injection. LRRK2 labelling was lightly detected in some neurons (Fig. 16C) and neurites (Fig. 16D) in the SN. GFAP labelling was observed in the SN on both side (Fig. 16E). Surprisingly, LRRK2-immunoreactive astrocytes were observed near the ipsilateral SN, in the pedunculus cerebri (Fig. 16F).

Dosage of dopamine into the striatum of 4 control HD-GFP and 4 HD-LRRK2* injected animals

Lemurs brains were rapidly removed and tissue dosages of monoamines (DA, 5-HT) and their metabolites (DOPAC, HVA, 5-HIAA) were performed.

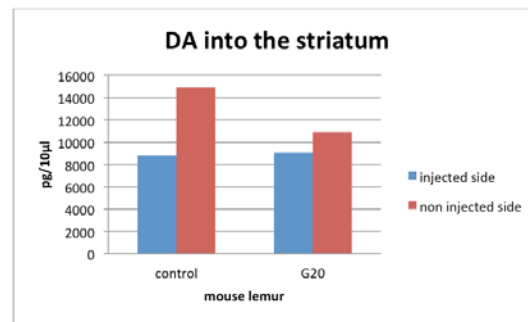


Figure 17: Dopamine level into the striatum of mouse lemurs

The injection into the striatum of 2×10^9 physical particles of HD-LRRK2 and HD-GFP have clearly an impact of the dopamine level of the striatum whatever the vector injected (Fig.17). The dopamine content is not significantly changed depending on the virus injected into the striatum. However the injection into the ipsilateral side in the G2019S lemurs involved a decrease of the dopamine level in the contralateral side. This decrease is not observed in the control animal suggesting that it is an effect of the LRRK2 expression.

Level of dopamine into the SN of control, WT, and LRRK2* lemurs

We have done mapping of TH-immunoreactive neurons into the SN of 4 controls, 4 Wild type and 8 LRRK2* (G2019S) and counted the number with the software Mercator (Explora Nova) (Fig. 18).



Figure 18: Mapping of TH-immuno-reactive neurons into the SN of a G2019S lemur

We observed a weak loss of TH neurons in the SN in the ipsilateral side whatever the virus injected (Fig. 19). But we observed also a decrease in the contralateral side in LRRK2WT and LRRK2* compared to control suggesting a role of the overexpression of the LRRK2 gene. This is in agreement with the results observed into the striatum. We need to investigate the number of neurons into the SN in non-injected lemurs to confirm this result.

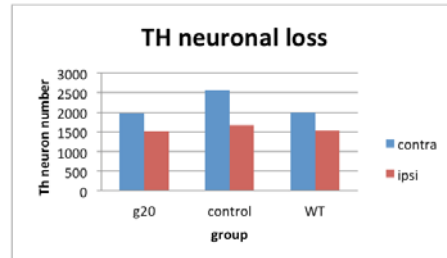


Figure 19: Evaluation of dopaminergic neuronal loss into the contralateral and ipsilateral SN of mouse lemurs.

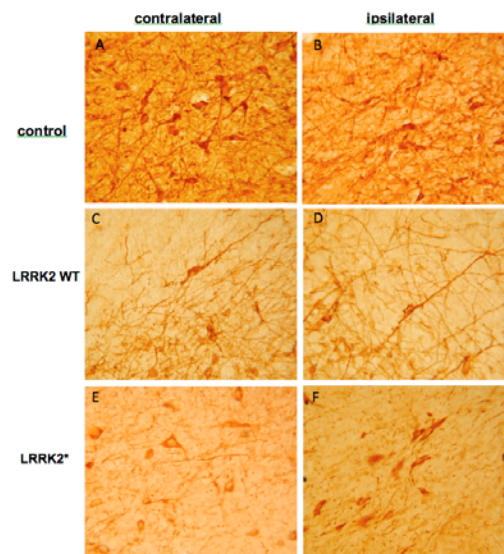


Figure 20: Labelling of TH-immunoreactive neurons into the different groups of mouse lemurs

Morphology of the dopaminergic neurons in the SN

We detected a loss of dopaminergic fibers in G2019S animals compared to control and wild type animals (Fig. 20). We observed dystrophic neurites and swollen axons, characteristic of neurodegeneration (Fig. 21C).

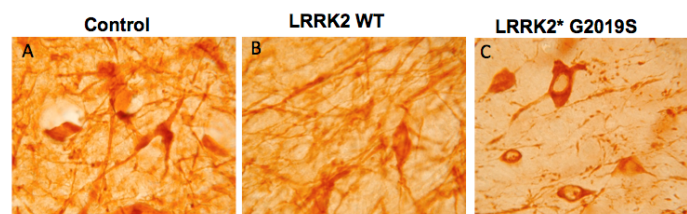


Figure 21: morphology of dopaminergic neurons into the nigra of mouse lemurs

Summary: The injection of HD-CAV-LRRK2* into the striatum of mouse lemurs leads to transient motor deficits in prehension, postural stability and rigidity of the body. The loss of dopaminergic neurons is weak but we observe a clear decrease of the number of fibers and apparition of swollen axons and dystrophic neurons, characteristic of neurodegeneration. We observe also a glial activation on the ipsilateral SN. 6 months postinjection into the striatum, this suggested that the HD-LRRK2* lemurs present early signs of PD.

D4.6: Report describing HD-LRRK2* vector efficacy in *Macaca fascicularis*

Injection of HD-LRRK2*

We performed a pilot study in two Macaques to determine the distribution and axonal transport of CAV-2 into the monkey brain.

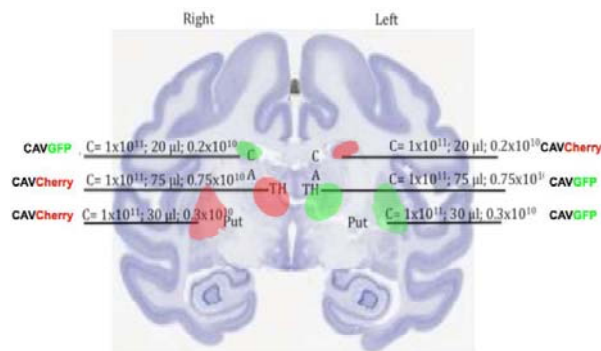


Figure 22. Strategy for comparison of conventional and CED based delivery of CAV-2 vectors in the Macaque brain. Coordinates for injection were calculated based on MRI images. Vector concentration was adjusted at 1×10^{11} physical particles/ml and the infused volume is reflected

Stereotaxic delivery of CAVGFP and CAVCherry was performed into the caudate nucleus, putamen and thalamus of 2 intact animals. Convection enhanced delivery (CED) was used for putamen and thalamus injection while the injection into the caudate nucleus was undertaken by conventional method. GFP and Cherry expression were found throughout the brain. We observed no obvious advantage for CED versus conventional delivery.

GFP-expressing cells were detected in the homolateral SN indicating that CAV2 can be effectively transported from the injected site to projecting areas. However, we found very few GFP-ir cells in the homolateral SN. These results indicate that CAVGFP can be efficiently transported into the monkey brain. Since the injected volume (target failure) and the number of cells expressing CAV2-GFP in afferent brain regions were very small we conducted another pilot study in 2 monkeys. In this case, monkeys we injected with 30µl of CAV2-GFP in the motor area of the putamen ($10e^{11}$ pp/ml), which resulted in transduction of 47% of the total striatum. All cells transduced by CAVGFP in the SN were neurons and the infusion of CAV2-GFP into the putamen provoked a widespread expression of GFP in

different brain areas (cortex, thalamus, SN). In addition, CAV-2 vectors induced an activation of microglial cells in the injected and transduced brain areas. We also found a 15% of neuronal loss in the homolateral SN when compared to the contralateral side. However, we found 30-40% neuronal loss in both SN when compared to the intact animals.

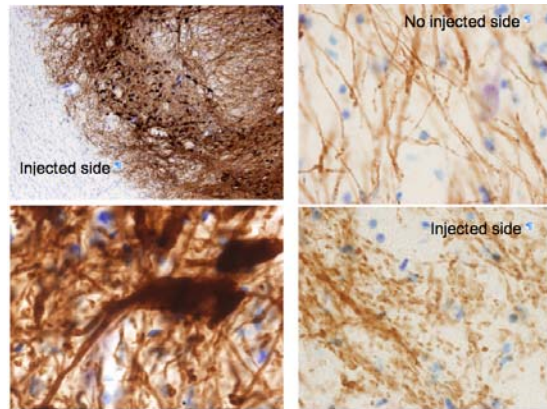


Figure 23 injected monkeys

Then, we injected HD-LRRK2* (G2019S) in 4 monkeys. $10e^{10}$ total particles were injected into two different sites of the left putamen. Six months after the surgery animals showed no behavioral changes either in motor activity or in the performance of fine motor tasks. Only a mild and inconsistent postural tremor of the right limbs was observed soon after CAV2 injection that was maximal 3 months after the surgery.

Functional imaging studies showed 20% decreased striatal DTBZ uptake in the injected striatum. Reduction of the total striatal DTBZ uptake was evident as soon as 15 days after surgery and remained over 6 months. In the caudate and putamen the reduction of DTBZ uptake was observed 15 days after surgery while in the posterior putamen the DTBZ uptake was progressively reduced over the time.

Histological analysis showed reduced density of dopaminergic neurons in the homolateral SN. As compared to intact SN, the number of TH-ir and VMAT-ir neurons was bilaterally reduced by 20% but the difference was not statistically significant. Notably, we found morphological changes in SN neurons consisting of dystrophic neurites and broken and swollen axons that were more evident in the homolateral SN. Electron microscopy studies are ongoing to confirm these changes. A weak FLAG labeling was found only in the putamen and around the injection site. Extracellular LRRK2 staining was present in the homolateral putamen, thalamus and SN.

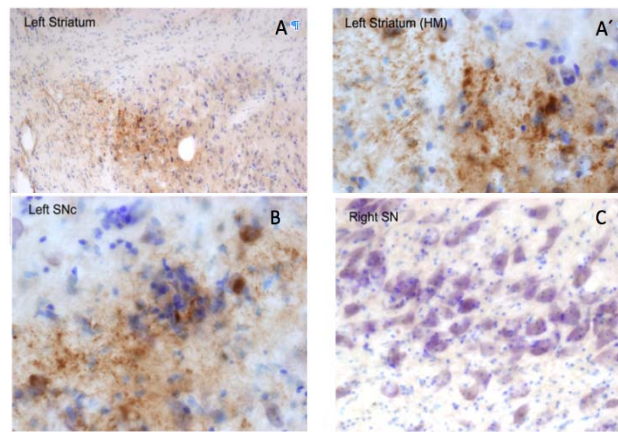


Figure 24 Tyrosine hydroxylase immunostained section of the SN of one monkey injected with HD-LRRK2* into putamen to illustrate morphological changes. LRRK2 immunostained section to illustrate the extracellular expression of LRRK2 in the site of injection (A), a high magnification of left putamen (A'), homolateral SN (B) and contralateral SN (C).

To indirectly assess the expression of LRRK2 in the SN, we looked for the existence of phospho-Tau in the homolateral brain structures since some studies have showed that LRRK2 overexpression might increase kinase activity and protein phosphorylation. Increased p-Tau staining was detected in both hemispheres of the 4 HD-CAV2-LRRK2* injected animals but it was more evident in the injected side.

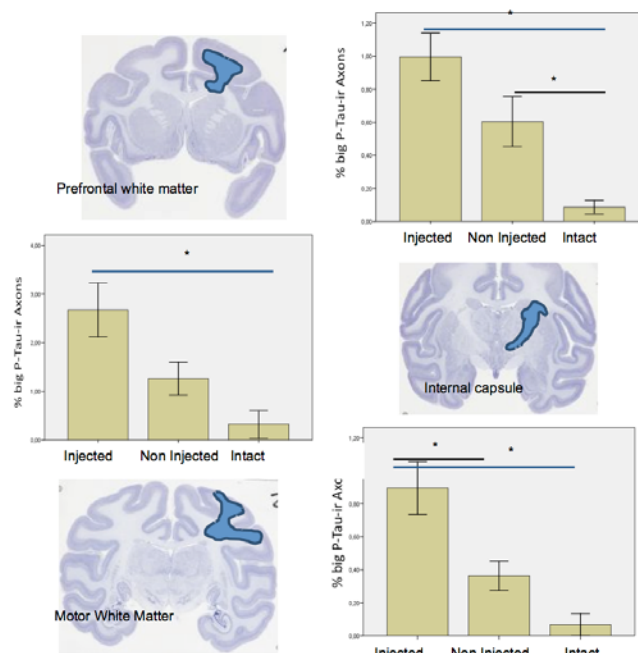


Figure 25. Quantification of p-Tau immunostaining intensity in the different brain structures. Note the significant increased intensity of p-Tau in the white matter of the injected side

Corrective action: Because striatal injections did not induce significant behavioral and histological changes, we then performed CAV-2 nigral injections.

We first injected the first generation (1G)-CAV2-GFP vectors in 2 monkeys as a pilot study. The injection was performed in both SN (10^9 pp per side) and the animals were sacrificed 4 weeks later.

In these animals we found a large number of GFP-ir cells in both SN (62% in the right and 74% in the left) and we detected 30-40% nigral cell loss. GFP expression was evident in other nigral projecting areas, like orbital and motor cortex, hypothalamus, caudate, and midbrain nucleus (Figure 26)

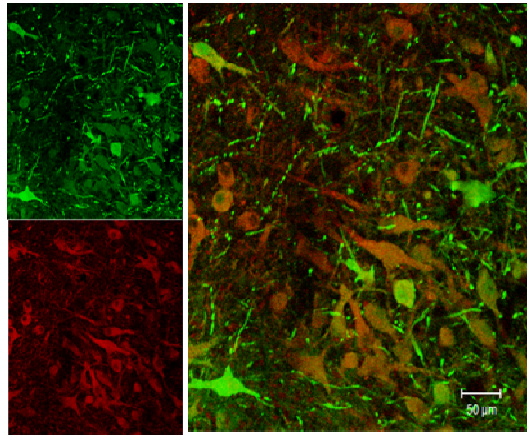


Figure 26. Confocal microphotograph of SN. In red TH-ir cells and GFP-ir cells in green.

Finally, we performed unilateral nigral injection with HD-CAV2-LRRK2* in 4 monkeys (10e10 total particles). Four additional monkeys were injected with HD-CAV2-GFP. Motor abnormalities were not observed in any animal during the 12 months of follow-up. Functional imaging studies showed no significant differences in the striatal DTBZ uptake with respect to basal value in both group of animals (LRRK2* and GFP).

When compared to the non-injected side, both groups showed 10-20% reduction in the DTBZ striatal uptake 12 months after surgery. The DTBZ striatal uptake showed wide differences among animals of the same group and we did not find any evidence of progressive loss of striatal DTBZ uptake. All animals (3 HD-CAV2-LRRK2* and 3 HD-CAV2-GFP) were sacrificed 12 months after surgery. One animal of each group was lost during the the follow up. One animal died 15 days after surgery due to a surgery-induced complication and the other died 6 months after surgery because of anesthetic reaction. Histological analysis showed the correct placement of the injection (right SN) in all animals. We did not observe any morphological change of in TH-ir cells either in the soma or neurites (Figure 27).

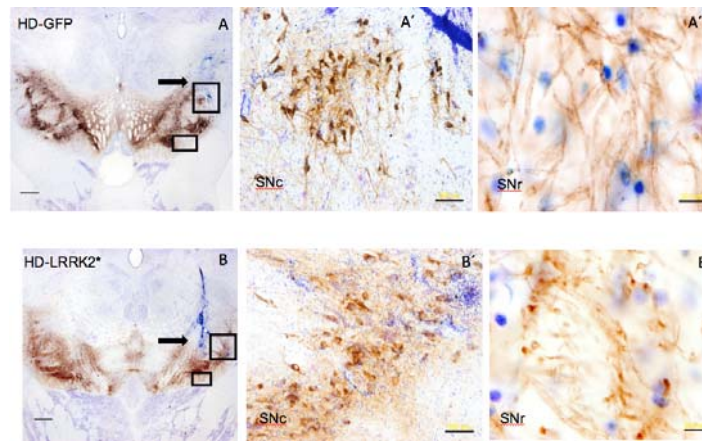


Figure 27. Photomicrograph of TH immunostained sections of SN to illustrate the site of injection (black arrows) in one animal injected with HD-CAV2-GFP (A) and in another injected with HD-CAV2-LRRK2* (B). High magnification of SNpc (A' and B') and a high magnification of SNpr (A'' and B'').

In these animals we found a bilateral reduction in the density of nigral dopaminergic neurons (10% approximately) when compared to intact animals. The number of TH-ir cells in the SN was similar in the injected and not injected side. In addition, both groups of animals exhibited a similar number of TH-ir cells.

Summary:

- CAV-2 was efficiently transported in a retrograde manner in the monkey brain and it showed a neuronal selectivity
- CAV-2 delivery into the brain induced the overexpression of GFP and LRRK2* proteins in brain areas projecting to striatum
- HD-LRRK2* injection into the putamen induced a loss of striatal 11C-DTBZ uptake and dopaminergic cell loss (VMAT-ir cells) in the homolateral SN
- HD-LRRK2* injections into the putamen induced overexpression of LRRK2* into the SN cells and provoked damage of the axons and neurites but no parkinsonism
- HD-LRRK2* injection into the striatum induced increased levels of phosphorylated Tau protein in several brain structures of the homolateral hemisphere.
- Striatal injections HD-LRRK2* induced gliosis and microglial activation in striatum and SN even 6 months after vector injection
- HD-LRRK2 and HD-GFP injection into the SN does not induce any behavioral manifestation 12 months after the surgery
- The decreased density of dopaminergic nigral cells observed after HD-LRRK2 and CAV-2 GFP delivery into the SN may be related to the vector injection itself

WP 5: Production and purification of HD CAV-2 vectors

D5.1 MDCK-E1-Cre recombinase cell line

An MDCK-E1-Cre recombinase cell line for the amplification of CAV-2 derived vectors was established from MDCK from ECACCC (No 84121903, lot 05G029). The cells were maintained and genetically modified in MEM 10% (v/v) FBS, full traceability records of the animal origin reagents used were retained.

Starting with MDCK cells, MDCK-E1-Cre cells were created in a 2-step procedure to constitutively express the CAV-2 E1 region and Cre recombinase. In step 1, MDCK cells were transfected with a plasmid called pCI-neoE1K9 provided by Partner 1-CNRS. pCI-neoE1K9 contains a CAV-2 E1 region expression cassette and a neomycin resistance gene. These cells (MDCK-E1) were selected with G418 and cloned by limiting dilution. E1 expression was functionally screened by the clone's ability to amplify E1-deleted CAV-2 vectors. A high E1-expressing MDCK-E1 clone was then transfected, in step 2, with a plasmid called pZeoCre (provided by Partner 1-CNRS), which expresses an nls-Cre recombinase and Zeocin resistance genes. After transfecting the MDCK-E1 cells with pZeoCre, potential MDCK-E1-Cre clones were selected for Zeocin resistance and limiting dilution. Cre recombinase activity was indirectly screened by the ability of the cells to cleave a loxP-stop-loxP cassette upstream of a luciferase expression cassette. High expressing MDCK-E1-Cre clones were selected and are available. Cre expression was also screened by western blot analysis.

MDCK-E1-Cre cells are available and will be tested for production of HD CAV-2 vectors (currently under development by consortium partners CNRS and UAB).

D5.2: Report describing set-up of differential packaging system

The goal of **D5.2** was to generate a CAV-2 vector that contained one of the phiC31 recombinase recognition sequences (attB) near the packaging signal and determine if this sequence, as in the case of human adenovirus serotype 5, delayed the production of mature CAV-2 particles.

CNRS designed a 1 kb sequence that contained the inverted terminal repeat (ITR), lox61, attB, a mutated packaging signal (based on CAV4.19, Soudais et al Mol Ther 2001) and lox67. The lox61 and lox67 sequences were chosen to avoid reinsertion of the excised floxed sequence into CAVattBCherry during the final step of HD (HD) vector production. This sequence was synthesized, and sub-cloned upstream to a Cherry expression cassette in pTCAV-12VK. The resulting construct, pTCAVattBCherry was recombined with pTG5412, which contains the entire CAV-2 genome, to create a plasmid (pCAVattBCherry) that harboured the E1-deleted vector genome of the CAVattBCherry. CAVattBCherry was removed from the plasmid and transfected into DKZeo cells to produce the vector.

During the amplification it became obvious that CAVattBCherry had a delayed production of mature particles: the amplification cycles were optimal after collecting the cells 4-5 days post-infection instead of

the normal 36 hours cycle for CAV-2. CAVattBCherry amplification was not only slower, but also less efficient, likely due to the incorporation of the mutated packaging signal. These characteristics are difficult for production, but optimal for CAVattBCherry use as a helper vector for HD vector production. Post-vector purification, CNRS and UAB tested the packaging delay using CsCl purified vectors via FACS and limiting dilution assays. Both assays showed that CAVattBCherry has a delayed packaging. Restriction digestion of vector DNA purified from infected DKZeo and DKCre cells showed that the genome is also sensitive to Cre recombinase removal of the packaging domain.

Conclusion: D5.2 completed successfully and *BrainCAV* has generated a CAV-2 helper vector with characteristics that are optimal for HD vector production.

D5.3 Optimized bioreactor protocol

This technical deliverable described the optimized procedure for the cultivation of MDCK E1 cells adapted to serum-free medium and the production of CAV-2 vectors using a stirred tank bioreactor. The protocol also supports the procedure for production of HD (HD) CAV-2 vectors.

D5.5 Helper and HD master virus bank and GMP master cell bank

Helper and HD virus banks were manufactured in April 2011 and May 2012, respectively. Δ E1 helper vector, denominated as JBA5, contains loxP sites flanking packaging domains and a RSV-lacZ expression cassette. For JBA5 master virus bank, DKZeo cells maintained in DMEM supplemented with 10 % (v/v) fetal bovine serum and 1% (v/v) of non-essential amino acids were infected with MOI 5. Viral vectors were harvested 48 hpi and purified by CsCl₂ gradients. Thirty vials, 500 μ l each, of Helper vector JBA5 in phosphate buffered saline with 10% (v/v) glycerol were produced and stored at -85°C in the premises of partner 4. HD vector denominated as HD-GFP, contains an GFP expression cassette. HD-GFP bank was prepared after infecting DKCre cells in same culture medium using an MOI ratio between HD-GFP and JBA5 of 5 to 1. Vectors were harvested and purified. 36 vials, 500 μ l each, of HD-GFP in PBS with 10% (v/v) glycerol were produced and stored at -85°C in the premises of partner 4. JBA5 were also banked after purification using an optimized purification protocol based in chromatographic steps using 1L bioreactor bulk treated with 50 U/mL of benzonase as starting material (more details are described in Deliverable 5.3 and Deliverable 5.4). Briefly, in this protocol, the clarification step is composed by centrifugation at 10000 g during 15 min followed by microfiltration using Sartopure 2 membrane capsule made of polyethersulfone (Sartorius Stedim Biotech); intermediate purification is performed by anion exchange chromatography using monolithic column; finally, a polishing step, to maximize the removal of impurities using a Captocore bead prototype from GE Lifesciences was performed. Using this protocol, approximately 1×10^{10} infectious particles (IP) or 2×10^{11} physical particles (PP) were obtained in 67 ml. Each vector bank was controlled by quantifying IP and PP. Titration of infectious JBA5 vectors was based in lacZ gene expression and β -galactosidase activity, while quantification of

infectious HD-GFP was performed by monitoring the expression of GFP. Physical particles and JBΔ5 contamination were quantified.

GMP master MDCKE1Cre cell bank:

A GMP-certified Master Cell Bank (MCB) for MDCK-E1 Cre was manufactured in February 2012 using the procedures described in the Batch Production Record PF-012. The manufactured MCB batch number is 00412.

The QC tests used for the approval and release of the GMP-certified MDCK-E1 Cre Master Cell Bank were defined according to the European Pharmacopoeia. 100 vials with, 1 mL each, of the GMP-certified MDCK-E1 Cre Master Cell Bank were produced. They are stored in the vapor phase of liquid nitrogen. Process details are described in the Batch production record (PF-012).

WP 6: Dissemination and transfer of knowledge

WP6 (WP leader EJ Kremer CNRS) addressed the need to inform scientists, health care professionals, the general public, patient associations, and families about the initiative of the European Union via **BRAINCAV**.

Scientists:

BrainCAV generated the following publications:

- Henaff D., E. Seiradake, H. Wodrich, O. Billet, M. Perreau, C. Hippert, F. Mennechet, G. Schoeh, H. Lortat-Jacob, H. Dreja, S. Ibanes, V. Kalatzis, J.P. Wang, R.W. Finberg, S. Cusack & **EJ Kremer. 2009** The cell adhesion molecule CAR & sialic acid on human erythrocyte influence adenovirus biodistribution. *PLoS Pathogens* Jan;5(1):e1000277.
- Salinas S, Bilsland L, Henaff D, Weston AE, Keriell A, Schiavo G & **EJ Kremer. 2009.** CAR-associated vesicular transport of an adenovirus in motor neuron axons. *PLoS Pathogens* May;5(5):e1000442.
- Lau AA, Hopwood JJ, Kremer EJ, Hemsley KM. **2010** SGSH gene transfer in mucopolysaccharidosis type IIIA mice using canine adenovirus vectors. *Mol Genet Metab.* 100(2):168-75
- Lau AA, T Rozaklis, S Ibanes AJ Luck H Beard S Hassiotis K Mazouni JJ. Hopwood, EJ. Kremer & KM Hemsley. **2012** Helper-dependent canine adenovirus vector-mediated transgene expression in a neurodegenerative lysosomal storage disorder *Gene* 1;491(1):53-7
- Salinas S & EJ Kremer. **2012** Virus induced & associated post-translational modifications. *Biol Cell.* 04(3):119-20.
- Brito C, Simão D, Costa I, Malpique R, Pereira CI, Fernandes P, Serra M, Schwarz J, Kremer EJ & Alves PM. **2012** Generation and genetic modification of 3D cultures of human dopaminergic neurons derived from neural progenitor cells. *Methods* Mar;56(3):452-60.
- P Fernandes, C Peixoto, VM Santiago, EJ Kremer, AS Coroadinha & P Marques Alves. **2012** Bioprocess development for canine adenovirus type 2 (CAV-2) vectors. *Gene Therapy* Jul 5. doi: 10.1038/gt.2012.52
- Fernandes P, Santiago VM, Rodrigues AF, Tomás H, Kremer EJ, Alves PM & Coroadinha AS. 2013 Impact of E1 and Cre on Adenovirus Vector Amplification: Developing MDCK CAV-2-E1 and E1-Cre Transcomplementing Cell Lines. *PLoS ONE.* 2013;8(4):e60342. doi: 10.1371/journal.pone.0060342.

- Salinas S, Schiavo G & **EJ Kremer**. **2010**. A hitchhiker's guide to the nervous system: the complex journey of viruses and toxins. *Nature Reviews Microbiology* Sep;8(9):645-55.
- Bru T, S Salinas & **EJ. Kremer**, **2010** An update on canine adenovirus type 2 and its vectors. *Viruses* 2, 2134-2153; doi:10.3390/v2092134
- Henaff D, S Salinas & **EJ. Kremer**, **2011** An adenovirus traffic update: from receptor engagement to the nuclear pore. *Future Microbiology* 2011 Feb;6:179-92.
- Henaff D & **EJ Kremer**. **2008** Adenovirus hexon mediates liver gene transfer (Tropisme in vivo de l'adénovirus – rôle inattendu de l'héxon). *Medicine & Science*. Aug-Sep;24(8-9):673-5.
- Segura MM, Monfar M, Puig M, Mennechet F, Ibanes S, Chillón M. A real-time PCR assay for quantification of canine adenoviral vectors. *J Virol Methods*. **2010** Jan;163(1):129-36.
- Henaff D, Salinas S. An endocytic CARriage tale: Adenoviruses internalization and trafficking in neurons. *Virulence*. **2010** May-Jun;1(3):188-91.

In addition poster presentations were done every time possible with a special effort during the final dissemination event organized within the 2012 ESGCT meeting in Versailles with a total of 13 posters presented at this occasion and covering all aspects of the **BRAINCAV** work:

- P. Alves Marques, A. Baker, A. Bosch, M. Carrondo, EJ Kremer, I. Saggio, J. Schwarz, G. Schiavo, JM Verdier BrainCAV: a nonhuman adenovirus vector for gene transfer to the brain P286
- C. Brito, D. Simaoa, I. Costa, R. Malpiquea, C. Pereiraa, P. Fernandes, M. Serraa, SC. Schwarz, J. Schwarz, EJ Kremer, P. Alves. Generation and genetic modification of 3D cultures of human dopaminergic neurons derived from neural progenitor cells. P287
- L. Ariza, A. Cubizolle, M. Chillon, N. Serratrice, EJ. Kremer, A. Bosch. Helper-dependent CAV-2 vector corrects neuronal pathology in a mouse model of mucopolysaccharidosis type VII P288
- P. Fernandes, C. Peixoto, VM. Santiago, EJ. Kremer, AS. Coroadinha, P. Alves Marques. Bioprocess development for canine adenovirus type 2 vectors P289
- G. Devau, E. Chazot, N. Mestre-Frances, EJ. Kremer, JM. Verdier. Canine adenovirus type 2 (CAV-2) transduction induces two different responses at 24h and 28 days in the brain of the nonhuman primate *Microcebus murinus*. P290
- C. Edwards, AC. Bradshaw, R. Burchmore, AH. Baker. Analysis of human serum interactions with Ad5 and CAV-2: a proteomic approach. P291
- MM Seguraa, M. Monfar, M. Puig, F. Mennechet, S. Ibanes, M. Chillon. A real-time PCR assay for quantification of canine adenoviral vectors. P292
- S. Salinas, LG. Bilsland, D. Hénaff, AE. Weston, A. Keriell, GP Schiavo, EJ Kremer. CAR-associated vesicular transport of an adenovirus in motor neuron axons. P293
- S. Piersanti, L. Astrologo, V. Licursi, R. Negri, E. Roncaglia, E. Tagliafico, EJ. Kremer, I. Saggio. Canine adenovirus (CAV-2) vectors induce an innate immune response and the modulation of cell cycle genes in dopaminergic differentiated human midbrain neuronal precursors. P294
- N. Serratrice, N. Mestre-Frances, S. Salinas, N. Bayo-Puxan, T. Bru, C. Zussy, F. Mennechet, S. Ibanes, A. Cubizolle, M. Perreau, V. Kalatzis, JM. Verdier, EJ. Kremer. Widespread and long-term expression in the primate CNS using helper-dependent canine adenovirus vectors. P295
- Cubizolle, N. Serratrice, A. Gennetier, S. Ibanes, ME. Haskins, EJ. Kremer. Helper-dependent CAV-2 injection into the CNS of mucopolysaccharidosis type VII dogs. P296
- P. Fernandes, EJ. Kremer, AS. Coroadinha, PM. Alves. Production of helper-dependent canine adenovirus type 2 (CAV-2) vectors for gene therapy: impact of transcomplementing gene products on producer cell-line. P297

- MM. Segura, M. Puig, M. Chillon. Chromatography purification of canine adenoviral vectors P298.

Health care professionals:

Part-1 CNRS recently presented **BRAINCAV's** goals to the University Hospital in Montpellier on period 1.

General public:

Part-1 participated in British Society of Gene Therapy public engagement day (March 29th 2010) to talk about **BRAINCAV's** goals in for brain therapies. Part-4-IBET participated in a public engagement day at ITQB.

Patient associations: Part-1 is in regular contact with the French lysosomal storage disorders society (VML) to communicate **BRAINCAV's** goal to its members. Part-5 is in regular contact with the Spanish MPS society concerning three MPS VII children in Spain.

Expected results, potential impact and use

Due PD's prevalence, the greatest socio-economic impact **BRAINCAV** could have is for the understanding and treatment of Parkinson's disease. Over 1 million Europeans suffer from Parkinson's disease with 40% of the victims under the age of 60. Parkinson's disease costs the EU over 50 billion € annually in health care, disability, loss of productivity, and long-term care - a cost that will only increase as the population ages. At present ~1% of the population >50 years old has Parkinson's disease. This number will increase in concert with the number of older people. Since the submission of **BRAINCAV**, the use of CAV-2 vectors in the context of PD (fundamental and clinical applications) has attracted significant interest from the scientific community. Numerous colleagues have contacted **BRAINCAV** members. Recently, there has been a North American led initiative to invest in better PD animal models. **BRAINCAV's** WP4 is therefore primed to make a significant contribution in this respect.

The global financial impact is lower for lysosomal storage disorders that affect the brain. However, the burdens place on the families and health care system are far from negligible. WP 3's goal to treat MPS VII, an extremely rare disorder, will carry-over to many lysosomal storage disorders caused by defects in soluble lysosomal enzymes.

The outcomes from **BRAINCAV** will have numerous applications for other major human health issue and indirect uses (vaccination of domestic animals and livestock). For example, clinical grade CAV-2 vaccine vectors will be possible due to GenIBET's GMP quality cell line.

When **BRAINCAV** was written, our *esprit* was that it was a "nuts & bolts" systematic approach to develop and test CAV-2 vectors. The partners in **BRAINCAV** showed their ability to develop simple questions and approaches into elegant studies. This is highlighted by the **BRAINCAV**-funded studies published. Therefore, **BRAINCAV's** scientific impact has already begun to be felt.

WP 0: Management

Consortium management tasks and achievements

The Project Manager assumed the follow-up of the Grant Agreement signature between the EC and the coordinator CNRS, providing all necessary information/documents to both parties. Initially scheduled on September 2008, the GA was finally signed December 18, 2008. (With the authorization of the EC Project Officer, the project had started October 1st, 2008.) The manager also did a follow up of the GA accession forms to be established by the beneficiaries of the project. The EC funds were transferred to the coordinator end January 2009, and the Project Management team (Coordinator + Manager) processed with the administrative and financial follow-up of the distribution of the EC grant to the beneficiaries. All funds were distributed by beginning February 2009.

From the start of the project, the Manager has informed the consortium with all information/documentation useful to the project administration, either through e-mailing or the BrainCAV extranet. First of all, he sent a contact sheet to every beneficiary to enable exchanges between scientists. The Consortium agreement was discussed between all beneficiaries and finally signed by all beneficiaries on September 2009.

The Manager prepared the internet website (www.braincav.eu) with the scientific coordinator to inform a large public with all scientific news coming from the project. The website was updated each time necessary. The Project Management team also prepared the design for poster and leaflets to be used during events to inform about the project, either in English or translated in own beneficiary's language.

Regarding internal exchanges for both scientific and administrative purposes, the Manager installed a secured extranet platform on-line (www.extranet-braincav.eu) where any BrainCAV member can find all legal and IP issues, all scientific presentations showed at the meetings, and all material (info, guides, templates) useful for reporting.

Following the annex 1, several Annual meetings and ExB management meetings were organised in the course of the project here is the list of the meetings:

- The Manager organized the Kick Off meeting in Montpellier, taking in charge all logistics and communication tasks. The KO meeting was hold at Hotel Massane on October 13-14, 2008.
- First General Assembly meeting and Executive Board meeting took place during the KO meeting. A first Press Release was issued to the destination of the scientific community and the politics, both in French and in English.
- Second Executive board meeting was held using phone conference but due to bad communication conditions, it was cancelled and replaced by individual phone calls.

- The Manager also helped partner 4 - IBET to organize the first annual meeting in Lisbon on November 5-6, 2009, and led the third Executive Board meeting.
- the Manager helped P3 – UNIROMA organize the second and third annual meeting in Rome (from October 21st to 23rd 2010) and
- the Manager helped P8 – ULEI Leipzig to organize the 3rd annual meeting in Leipzig (from October 24th to 25th),
- Together with the annual General Assembly meeting, an ExB meeting took place in Rome on October 23rd 2010.
- A month 30 ExB meeting was organized by web conference on April 28th 2011.
- Together with the General Assembly meeting organized in Leipzig, the month 36 ExB meeting took place on October 25th 2011.
- A month 42 ExB meeting was organised by teleconference on April 16th 2012.
- A month 48 ExB meeting was organised by web conference on September 18th 2012.
- The final meeting organised in Sitges in February 22nd to 24th, 2013. At this occasion, no formal ExB took place, but an overview of the work achieved and the organisation of the report preparation was done with all the partners.

During ExB meetings, the WP leaders or their representatives in the ExB presented their WP extensively in the perspective of the research and the ability to reach the contractual elements: deliverables and milestones. At this occasion the WP leaders presented intermediate progress reports. Both progress reports and minutes for each of these meetings have been added in the corresponding deliverables D0.8 and D0.6.

The Manager updated the Internet website (www.braincav.eu) developed in Period 1. The intranet platform of the BrainCAV where the members can find all legal and IP issues, all scientific presentations showed at the meetings, and all material (info, guides, templates) useful for reporting has been updated too.

Report preparation

PMT has been heavily involved in the preparation of the 3 periodic and the final reports. The Manager provided the templates and sending reminders to the partners. Together with the Coordinator, all elements put on the online reporting tools set up by the European Commission (SESAM and FORCE) were controlled. This has led so far to a limited number of comments from the European Commission because the major issues were dealt with before submission of the report. In a second step, the PMT ensured that the comments and remarks of the **BrainCAV** Scientific Officer were addressed in the best delays.

Grant Agreement amendment

BrainCAV had to request 4 GA amendments to take in consideration the changes in the consortium. This included the following changes:

- As the coordinator CNRS actually employed personnel from Inserm, it was suggested to adjust the previous budget by diminishing the Inserm budget and increasing the CNRS budget. The manager prepared an amendment that was agreed by the EC on April 2009. Beneficiary 2 (CRUK) asked to receive the whole EC contribution at once, as its work was concentrated on the first period. After formal agreement by the EC project Officer, it was agreed to do so.
- Some beneficiaries to the project disagreed to provide the Project Manager with all information regarding the IP rules internal to their institutions as the deliverable was set as "PU" (public) when it was seen as strategic... The consortium then agreed to mark the deliverable as "RE" (restricted access) or "CO" (confidential).
- Name of Legal Entity Authorized Representative of CNRS has changed from M. Michel Portefaix to Mrs Ghislaine Gibello, since January 1st, 2009.
- To address technically difficult experiments, budget changes were agreed upon between the partners during the ExB meetings and validated by the partners:
- P5, who was responsible for mid-size HD vector production, has not been able to produce HD vectors. To date, P1 is the only partner that can make HD vectors, but did not budget resources to produce vectors for 4 years. After discussing possible options, P5 proposed to reallocate some of its EC contribution to the P1 so that the P1 can continue the production of the vectors. P5 sent an evaluation of the amount that could be reallocate to the P1. As a consequence, P5 EC contribution will be reduced by 17,680 € in favour of the P1; the initial EC request will not be otherwise modified. The P1 notes that this sum will not cover any related functioning costs and that it has already devoted extra resources to HD vector production during the first 30 months. At the M36 ExB meeting, P6 also offered to redistribute 20,000 € to P1 to ensure the production of the vectors. For similar reasons, the P8 will evaluate if a redistribution of its funding would be appropriate to support this production. The ExB members validated the proposed budget redistributions.
- Significant delays took place in the animal studies as explained in the RTD WP3 and 4 progress reports. This created an insurmountable problem into the ability to deliver on time. In spite of the alternatives explored to maximize the possibilities to stay within the limits of the initial work plan, it was not possible to deliver within 48 months. This was also foreseen as a major worry in the initial proposal. The animal studies were completed thanks to the 6-month extension of the GA. This lead to a 6-month extension, postponing the end of the project to month 54
- Departure of P8-ULEI from the Consortium

- Change in the Coordinator's contact
- Addition of the ICREA third party to P5-UAB
- Several limited changes to the Annexe 1 including the budget redistribution to take into account the departure of P8 and the redistribution of some tasks this partner was taking care of.

All these elements were changed in 4 GA amendments which were prepared for the coordinator by the manager and submitted by the coordinator.

Deviations from the original work plan and proposed corrective actions:

The main difficulties that occurred during the course of the project were solved or addressed by appropriate corrective action. The main issues were linked to the difficulties of working with MPS VII dogs and non-human primates. In addition, we had to deal with the departure of P8, who was WP4 leader and responsible for several tasks in WP4. P8 left the Consortium during the 3rd period and had to be replaced in order to ensure that the work could be finalized in the best conditions by the other *BrainCAV* participants. Tasks and budget had to be redistributed to ensure that P8 work could be finished in the best conditions and full respect of the initial workplan.

Thanks to the 6-months extension, all delays that appeared during the previous periods and especially those related to animal experimentation have been mostly recovered allowing *BrainCAV* to propose a very good level of achievement of its initial objectives. No deviation from the plan occurred after the 3rd and 4th amendments were implemented. No corrective actions to allow the delivery of the work were necessary.

Recapitulative effort table: Full duration

[illegible]

4.2 Use and dissemination of foreground

Section A

We performed a range of dissemination activities throughout the 4.5-year course of **BrainCAV**. Research strategies and results were communicated at the earliest possible stage, in accessible formats, within the consortium, to the scientific and industrial communities, and to the public, including targeted patient groups.

1. Dissemination within **BRAINCAV** was through electronic communication, an intranet platform and, general assembly meetings.
 - **Electronic communication** allowed an intern flow of information and helped day-to-day management of the consortium. Yearly video or teleconferences were organised to reinforce the exchanges.
 - **The extranet platform** distributed information (reports, manuals, Newsletters, events and templates) relevant to **BRAINCAV**. This platform also formed the basis of the public open project website.
 - **yearly General Assembly meetings** gathered the scientists involved in **BRAINCAV**. These meetings were an indispensable mean for integration and collaborative work.
2. Dissemination to the scientific and industrial communities was ensured through the website, peer-reviewed publications, and participation in congresses. This included meetings that also targeted primarily the business sector also (e.g. PDA meetings). The **BRAINCAV** website was opened to the public.

Numerous peer-reviewed publications have been published and many more will be submitted from **BRAINCAV**. Those published already are listed and uploaded in the appropriate places. Publication of our results in open access journals was encouraged. When not available as open access, the partners were encouraged to add to their home page to or in public available databases.

Scientific congresses typically form a principal information channel of any research community. We encouraged participation at gene therapy and brain related congresses, in particular

- meeting of the European Society for Gene and Cell therapy (ESGCT)
- meeting off the Federation of European Neurological Societies (FENS)
- meeting of the American Society of Gene Therapy (ASGT)
- MPS Conference and study group meetings
- Parkinson's disease conference
- ...as well as conferences and workshops at the national level

3. Dissemination to patient organizations and the greater public was ensured through at least five different

channels; (i) the VML (ii) the BrainCAV public web site, (iii) websites of each partner, iv) public awareness of science and gene therapy days, and v) a closing conference

- **Partner 1 was in regular contact with the VML**, a French lysosomal storage disease society that disseminates information relating to all issues relevant to people affected by lysosomal storage disorders. The actions of the **VML** followed four main themes:
 - finding a therapy,
 - Arranging international scientifics
 - Supporting the Health Services in improving the patients' quality of life
 - Increasing awareness through fund raising and broadcasting.

Partner 1 organized meetings with the **VML** to raise awareness of **BRAINCAV**-generated knowledge and to support use of our results.

- **The BRAINCAV public web site** contained non-confidential information, such as descriptions of the project and of the consortium partners and regular information on progress. Other items included downloadable versions of any publication or literature generated by the project. Moreover, each partner will inform the public about their participation in **BRAINCAV** through their own website to efficiently spread the information throughout Europe and even outside Europe. Finally, to close **BrainCAV** we sponsored a session at the 2012 ESGCT meeting in Versailles.

Section B

Plans for exploitation of acquired intellectual property

The **BRAINCAV** partners have significant experience in valuation of innovation; most partners have participated in the creation of start-up biotechnology companies, and/or hold positions as officers or consultants for such companies. Likewise, the **BRAINCAV** partners recognize that the crucial factor for valuation is the link between research-driven generation of technologies and know-how and the ability of companies to absorb the new IP and ensure that it is disseminated and translated into new therapies and clinical practice.

Two SMEs partake in the consortium. Each had a direct interest in the expected IP to be acquired, and thus could be immediately exploited. Since the interests of the SMEs are different but synergistic, competition and duplication will be avoided while the added value of collaboration and partnerships should accelerate the development process, from research efforts to candidate products, and render visible the positive nature of community research. However, while the consortium's SMEs do not present any conflicts of interest among them, they will be in direct competition with other companies, pursuing similar developments in the field. This is a challenge that must be seen as a positive and stimulating incentive to stay innovative and competitive.

The significant number of relevant patents held by the **BRAINCAV** partners insures that anteriority and freedom to operate has already been examined to a large degree. However, IPR value is strongly influenced by the novelty of the invention and the availability of alternative routes to the same solution.

BRAINCAV generated assets including:

- Cell lines capable of producing clinical grade CAV-2 vectors
- Helper vectors using the Φ C31 differential packaging system
- Helper-dependent CAV-2 vectors expressing GUSB and LRRK2
- Primates with early signs of Parkinson's disease
- Novel CAR tropism modified CAV-2 mutants
- 3D cellular cultures of human neurons

In accordance with the consortium agreement the IP belongs to the partner(s) generating it. When appropriate the IP capable of industrial or commercial application, the owner is in the process of provide for its adequate and effective protection. The consortium was regularly informed via the intranet platform about the advancement of the exploitable assets generated by the project. Whenever applicable, external companies were informed.